

The Electrical Conductivity of Aqueous  
Solutions of Strong Electrolytes at High Frequencies

Thesis by  
Kenneth Carl Crumrine

In Partial Fulfillment of the Requirements  
for the Degree of Doctor of Philosophy,

California Institute of Technology,  
Pasadena, California

1937

## Table of Contents

### Abstract

#### Chapter 1. Introduction

- Section 1.1 Purpose of research
- 1.2 Basic concepts of electrolytic conduction
- 1.3 Previous work in the field
- 1.4 Justification for the present research

#### Chapter 2. The experimental method

- Section 2.1 A simple resonance circuit
- 2.2 Another resonance circuit
- 2.3 Expression for resistance in terms of observables
- 2.4 The applicability of circuit diagrams
- 2.5 A circuit used extensively
- 2.6 Other circuits tested
- 2.7 Radiation resistance
- 2.8 Temperature correction
- 2.9 Test cell constants
- 2.10 Adjustment of circuit constants
- 2.11 Calculation of  $\Lambda_{\omega}$  from observables
- 2.12 An alternative method

#### Chapter 3. The apparatus

- Section 3.1 Oscillators
- 3.2 Resonance indicator system
- 3.3 Resonance circuit

#### Chapter 4. Test of the method and sources of error

- Section 4.1 Tests of the mathematical theory of the method
- 4.2 The selective heating effect
- 4.3 Other sources of error

#### Chapter 5. Results

- Section 5.1 Data
- 5.2 Conclusions

### Acknowledgments

### Bibliography

## Abstract

For the purpose of determining by an absolute method the electrical conductivity of aqueous solutions of representative 1 - 1 and 2 - 2 valent strong neutral salts over as great a range of concentrations and at as high frequencies as feasible, a new method, which is more general in applicability than the usual simple resonance method, has been developed, tested and used. Solutions of NaCl and MgSO<sub>4</sub> were studied at wave lengths of 45.5, 27.4, 16.4 and 4.04 meters. The concentration range covered the interval from 10<sup>-3</sup> to 1 gram equivalents per liter of solution. Fractional increases in the high frequency conductivity compared with the low frequency conductivity, considered as a function of the concentration with frequency constant, have been found to have a maximum of the order of 15% at approximately 10<sup>-2</sup> gram equivalents per liter of solution. This maximum shifted to greater concentrations as the frequency increased. The accuracy of the method was insufficient to show the small difference in high frequency conductivity of the two salt solutions having the same low frequency conductivity. Many relative methods have ascertained this difference, which is well predicted by the Debye-Falkenhagen theory. The results do not agree with the absolute values predicted by the theory for either salt in that concentration range (perhaps as great as 10<sup>-2</sup> gram equivalents per liter of solution) for which the theory was designed. For concentrations of the order of one normal, the results indicate only a small increase, if any, in conductivity at the frequencies employed.

Chapter 1. Introduction

## Section 1.1 Purpose of research

The purpose of this research was to determine the electrical conductivity of aqueous solutions of representative 1 - 1 and 2 - 2 valent strong neutral salts over as great a range of concentrations and at as high frequencies as feasible using the so-called simple resonance method.

## Section 1.2 Basic concepts of electrolytic conduction

A brief statement of the basic concepts of electrolytic conduction may be in order. The discovery of Faraday's law and the fact that electrolytic conduction obeys Ohm's law for ordinarily applied field strengths suggested the following expression for the equivalent conductivity  $\Lambda$  in terms of the specific conductivity  $\sigma$ , the concentration in milligram equivalents per liter of solution  $\gamma^*$ , Avogadro's number  $N$ , the electronic charge  $e$ , the ionic mobilities  $l_+$  and  $l_-$ , and the degree of dissociation  $\alpha$ :

$$\Lambda = \frac{10^6 \sigma}{\gamma^*} = \alpha N e (l_+ + l_-)$$

The equivalent conductivity  $\Lambda$  would be independent of the concentration if (1)  $\alpha$  were independent of the concentration and if (2)  $l_+$  and  $l_-$  were also independent of the concentration.

That one or the other or both of these assumptions is incorrect is well known. Arrhenius retained assumption (2) and rejected assumption (1). This classical theory of electrolytic solutions is quite successful for weak electrolytes, but leads to incorrect results for strong electrolytes.

If assumption (2) be rejected and assumption (1) retained, even for solutions as concentrated perhaps as 0.01 N, we are led to the following concepts of the Debye-Huckel-Onsager-Falkenhagen theory which is applicable to the present research for sufficiently dilute solutions.

We conceive of four different forces acting upon any individual ion in a solution. First there is the Stokes resistance. Second there is the force due to the applied electric field. Third there is the retarding force due to the ionic atmosphere of opposite sign to the charge on the central ion - which is aptly called the force of relaxation. And lastly there is the electrophoretic force due to the fact that the central ion moves thru a solvent which is not at rest relative to the container but which is being dragged in the opposite direction by the ionic atmosphere surrounding the central ion.

The mathematical application of these concepts to a study of the electrical conductivity of dilute solutions of strong electrolytes gave rise to the theory of dispersion of electrical conductivity (among other results) which is attributable to Debye and Falkenhagen.

This theory uses as a model of such a solution the concept of

small charged metallic spheres in a continuous viscous medium. It is applicable only to dilute solutions of strong electrolytes since complete dissociation is assumed and also because the charged spheres are likened to point charges in their electrostatic action on neighboring ions. (For a concentration of the order 0.01 N, the distance between ions is of the order of ten ionic diameters.)

Dispersion results at frequencies great enough such that dissymmetry of the ionic atmosphere occurs - an increase in conductivity is then expected because the retarding forces on the central ion become smaller. At still higher frequencies the conductivity ceases due to the inertia of the central ion and we arrive at the connection with the optical phenomenon of transparency of such a solution as NaCl in water.

It should be mentioned that the same model for an electrolytic solution which leads to the above conclusions concerning the dispersion of conductivity, also leads to the conclusion that at appropriate frequencies there will be an increase of the dielectric constant. However, in Debye's treatment\* of the dielectric constant of ionic solutions the effect known as electrical saturation played an important role. A consideration of such a model led Debye to the conclusion that the dielectric constant of an ionic solution should be somewhat less than the dielectric constant of the solvent.

\* Debye, Polar Molecules

### Section 1.3 Previous work in the field

Several methods have been used to test the Debye-Falkenhagen theory. Nearly all these methods are relative in character, the high frequency conductivity of  $\text{MgSO}_4$  for example being measured in terms of the high frequency conductivity of KCl solutions.

As early as 1927 M. Wien obtained evidence of the dispersion effect. Sack, however, was the first to obtain results of any accuracy at sufficiently high frequencies.

The method employed by Sack, Mittelstaedt and Brendel involved observation of the resonance current when a test cell was filled successively with a standard KCl solution and then with the comparison solution. The conductivities of solutions having concentrations of the order of  $10^{-3}$  or less gram moles per liter of solution were measured at wavelengths between 30 and 10 meters with an accuracy of the order of 0.2%. The dispersion effect predicted by the theory is of the order of 1% for these wave lengths. Agreement between experiment and theory was considered satisfactory for  $\text{MgSO}_4$ ,  $\text{CuSO}_4$ ,  $\text{K}_4\text{Fe}(\text{CN})_6$ ,  $\text{La}(\text{NO}_3)_3$ , HCl and  $\text{H}_2\text{SO}_4$ .

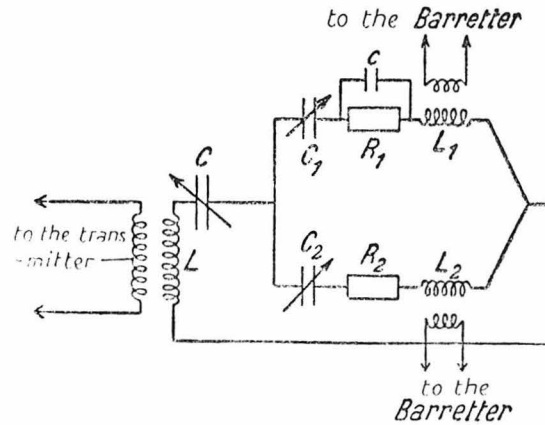
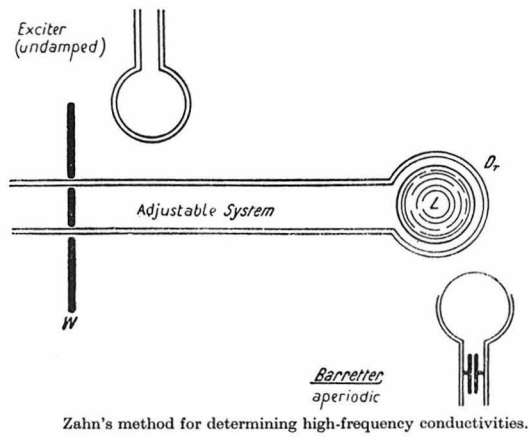
Deubner's method consisted of so adjusting a vacuum tube oscillator circuit that small changes in the conductivity of the solution filling a test cell in parallel with the principal capacitance produced large changes in the intensity of oscillation. A change in conductivity of 2% produced a change in galvanometer deflexion of 60 divisions. An accuracy of 0.03% is claimed. The effect predicted is of the order of

1%. Agreement with the theory was claimed, although small deviations were found.

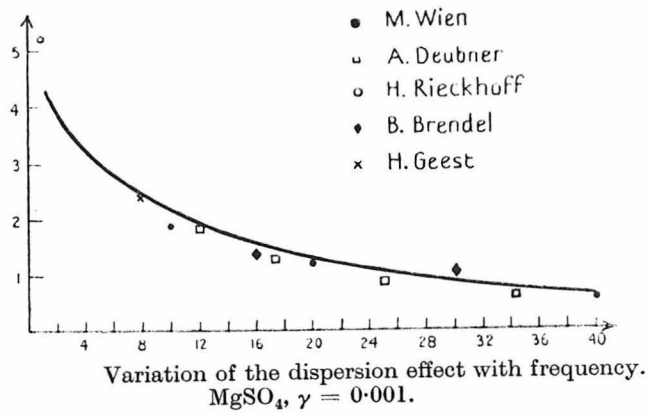
Zahn's method consisted in observing the effect due to losses in the test solution subjected to a high frequency magnetic field. A schematic diagram of his arrangement is shown at the top of the following plate\*: The data obtained for  $\text{MgSO}_4$  and  $\text{MnSO}_4$  in terms of KCl as standard at a wave length of about 1 meter are shown in Chapter 5. Agreement with the theory is claimed, the effect predicted being of the order of 10%.

M. Wien and his co-workers have used extensively a method which is evident from the following plate. A resonance curve plotting barretter deflection against  $C_1$  was first obtained using NaCl or HCl solution as standard in the test cell ( $c, R_1$ ). Using then a second electrolyte in the test cell, it was possible to obtain a second resonance curve identical with the first by altering  $R_1$  (changing the concentration slightly) and by altering  $c$ .  $\text{MgSO}_4$  and  $\text{Ba}_3 [\text{Fe}(\text{CN})_6]_2$  at concentrations of the order of  $10^{-2}$  and less gram moles per liter of solution were studied at wave lengths of 40, 20, and 10 meters. Again agreement with the dispersion theory is claimed.

\* This plate shows material selected from the English version of Falkenhagen: Electrolytes.



Wien's method for measuring conductivities and dielectric constants at high frequencies.



The methods so far mentioned are relative methods. A method described by Deubner and used by Malsch for solutions of  $\text{AgNO}_3$  and  $\text{FeCl}_3$  in  $\text{C}_2\text{H}_5\text{OH}$  is an absolute method. The test cell was converted into a thermometer by using a capillary and the rate of rise of liquid in the capillary was observed at high and low frequencies, the applied voltage being also observed. The data in Table 1.3 - 3 was obtained, agreement with the Debye-Falkenhagen dispersion theory being claimed.

Table 1.3 - 3

Solution	Moles per liter	$100 \frac{\sigma_\omega - \sigma_0}{\sigma_0}$		
		$\lambda = 76 \text{ m.}$	$\lambda = 48 \text{ m.}$	$\lambda = 28 \text{ m.}$
$\text{AgNO}_3$	1/300	0.2 + 0.5	0.1 + 0.5	0.9 + 0.5
$\text{AgNO}_3$	1/1000	0.6 + 0.5	0.2 + 0.5	0.7 + 0.5
$\text{FeCl}_3$	1/100	0.6 + 0.5	0.7 + 0.5	1.7 + 0.5
$\text{FeCl}_3$	1/300	0.3 + 0.5	0.3 + 0.5	0.6 + 0.5

The figure at the bottom of the accompanying plate shows the Debye-Falkenhagen dispersion curve  $\left( 100 \frac{\Lambda_\omega - \Lambda_0}{\Lambda_0} \text{ vs. } \lambda \right)$  for  $\text{MgSO}_4$  at  $18^\circ \text{C.}$  at a concentration of 0.001 gram moles per liter of solution. The points represent experimental data. The figure is due to Geest.

In the region of greater concentrations we may mention the results of Feldman given in Table 1.3 - 5 and of Smith-Rose given in Table 1.3 - 6.

Table 1.3 - 5

Specific conductivities at 21° C in number of 10<sup>-11</sup> e.m.u.

Sample	$\lambda = 130$ m.	100 m.	60 m.	35 m.	30 m.	23 m.	16 m.
Deep ocean water	4.4	4.4	4.4	4.6	5.0	5.0	5.2
Beach water				4.7		5.0	
3.5% NaCl		5.6		6.1			6.8
0.1 N KCl*		1.18		1.23			1.37

\* Handbook of chemistry and physics gives  $\sigma = 1.19 \times 10^{-11}$  e.m.u. at 21° C (14th ed., p. 944).

Table 1.3 - 6

Specific conductivity of sea water at 20°C.

Frequency (kc./s)	Conductivity (e.s.u. $\times 10^{-10}$ )
0.5	3.9
1.0	4.2
2.0	4.3
100.	4.3
1,200.	4.3
10,000.	5.4

Smith-Rose estimates that the accuracy of his data is about 5%. It

will be noticed that the quantity  $\frac{\sigma_{\omega} - \sigma_0}{\sigma_0}$  has the value 38% at  $\lambda = 30$  meters.

Section 1.4 Justification for the present research

For the purpose of this research the simple resonance method was chosen because it seemed to give promise of being an absolute method; not because it would give great accuracy, quick results, or even simplicity of application.

Unambiguous data obtained by this method would serve to test the Debye-Falkenhagen theory for dilute solutions, would satisfy scientific curiosity for concentrated solutions, and might possibly find application in connection with electrotherapeutics and geophysics.

## Chapter 2. The experimental method

In this chapter we shall proceed from a discussion of the simplest circuit, perhaps, which exhibits the phenomenon of series resonance to a discussion of a diagrammatic circuit which we assert bears some electrical resemblance to the apparatus used in this research. Although the mathematical expressions deduced from elementary alternating current circuit theory already are lengthy, they could easily be made longer if the circuit diagram should be made more complete. The writer believes, however, that many of the salient features of the apparatus are well represented by so simple a diagram as Figure 2.5 - 1 below. We shall derive a method in terms of this diagram for determining experimentally a resistance of the order of  $10^4$  ohms at frequencies of the order of  $10^7$  cycles per second. We shall mention the roles played by radiation resistance, temperature and test cell constants. Finally, we shall indicate the adjustments of circuit constants which are necessary to attain reasonable accuracy in the determination of high frequency conductivities.

### Section 2.1 A simple resonance circuit

It is convenient to consider first the circuit of Fig. 2.1 - 1.

We have the differential equation

$$\frac{d^2 I}{dt^2} + \frac{R}{L} \frac{dI}{dt} + \frac{I}{CL} = \frac{1}{L} \frac{dE}{dt}$$

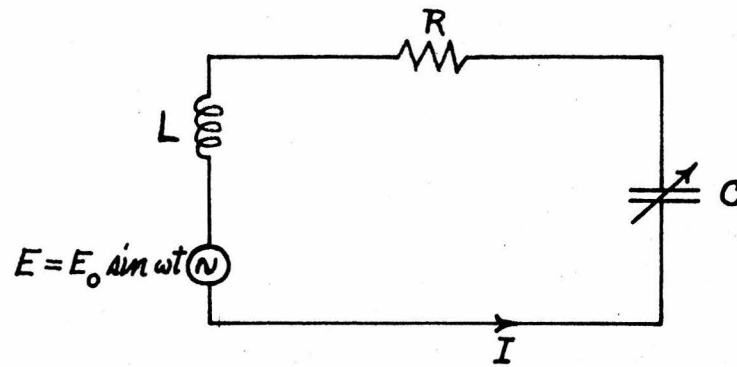


Fig. 2.1 - 1

of which the solution is

$$I = \frac{E_0}{\sqrt{R^2 + \left(L\omega - \frac{1}{C\omega}\right)^2}} \sin \left[ \omega t - \tan^{-1} \frac{L\omega - \frac{1}{C\omega}}{R} \right] +$$

$$A_1 e^{-\frac{RC + \sqrt{R^2 C^2 - 4LC}}{2LC} t} + A_2 e^{-\frac{RC - \sqrt{R^2 C^2 - 4LC}}{2LC} t}$$

From this we see that the resonant frequency is given by

$$\nu = \frac{\omega}{2\pi} = \frac{1}{2\pi\sqrt{LC}}$$

and the natural frequency by

$$\nu_0 = \frac{\omega_0}{2\pi} = \frac{1}{2\pi} \sqrt{\frac{1}{LC} - \frac{R^2}{4L^2}}$$

The logarithmic damping decrement is

$$\gamma = \frac{2\pi \frac{R}{2L}}{\sqrt{\frac{1}{LC} - \frac{R^2}{4L^2}}} = \frac{\pi R \sqrt{\frac{C}{L}}}{\sqrt{1 - \frac{R^2 C}{4L}}}$$

If we plot  $I^2$  against  $C$ , having varied  $C$  in the neighborhood of the resonance capacity  $C_r$ , we obtain a resonance curve as shown in Fig. 2.1 - 2

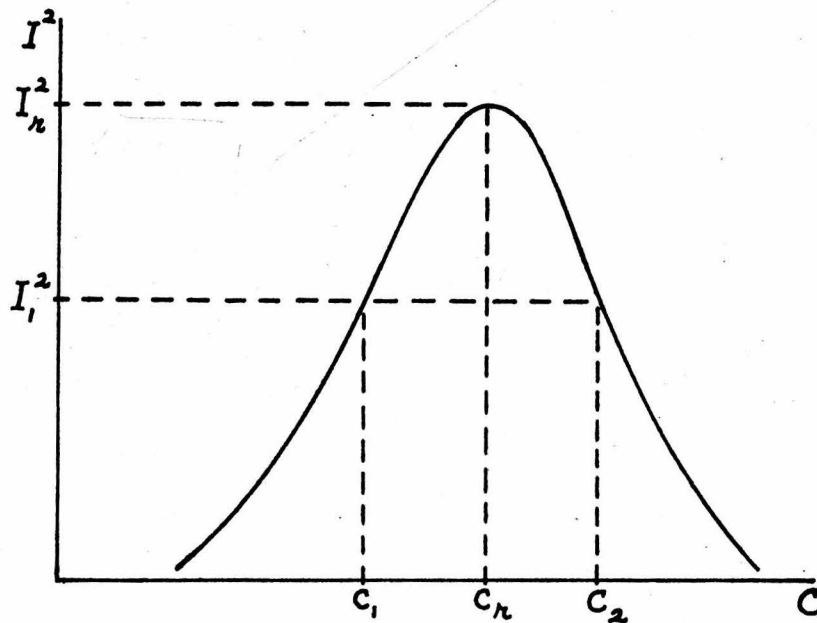


Fig. 2.1 - 2

We can now write:

$$I_n^2 = \frac{E_o^2}{R^2}$$

$$I_1^2 = \frac{E_o^2}{R^2 + \left(L\omega - \frac{1}{C_2\omega}\right)^2} = \frac{E_o^2}{R^2 + \left(L\omega - \frac{1}{C_1\omega}\right)^2}$$

$$\begin{aligned}
\left[ \left( \frac{I_n}{I_1} \right)^2 - 1 \right] 2R^2 \omega^2 &= \left( \frac{1}{C_1} - L\omega^2 \right)^2 + \left( L\omega^2 - \frac{1}{C_2} \right)^2 \\
&= \left( \frac{1}{C_1} - \frac{1}{C_n} \right)^2 + \left( \frac{1}{C_n} - \frac{1}{C_2} \right)^2 \\
&= \frac{1}{C_1^2} + \frac{1}{C_2^2} + \frac{2}{C_n^2} - \frac{2}{C_n} \left( \frac{1}{C_1} + \frac{1}{C_2} \right)
\end{aligned}$$

Making the approximations

$$\frac{1}{C_1} + \frac{1}{C_2} = \frac{2}{C_n} \quad \text{and} \quad \frac{1}{C_1^2} + \frac{1}{C_2^2} = \frac{4}{C_n^2} - \frac{2}{C_1 C_2} \quad \text{we have}$$

$$\left[ \left( \frac{I_n}{I_1} \right)^2 - 1 \right] 2R^2 \omega^2 = \frac{2}{C_n^2} - \frac{2}{C_1 C_2} = \frac{2}{C_n^2} \left( 1 - \frac{C_n^2}{C_1 C_2} \right)$$

or

$$R\omega = \frac{1}{C_n} \frac{\sqrt{1 - \frac{C_n^2}{C_1 C_2}}}{\sqrt{\left( \frac{I_n}{I_1} \right)^2 - 1}}$$

In those cases for which it is sufficiently accurate to use

$$\gamma = \pi R \sqrt{\frac{C}{L}} = \frac{\pi R}{L\omega} = \pi C_n R\omega$$

we shall have

$$\begin{aligned}
\gamma = \pi R \sqrt{\frac{C}{L}} &= \left[ \frac{\pi}{2} \frac{C_2 - C_1}{C_n} \frac{1}{\sqrt{\left( \frac{I_n}{I_1} \right)^2 - 1}} \right] \cdot \\
&\quad \cdot \left[ \frac{2C_n}{C_2 - C_1} \cdot \sqrt{1 - \frac{C_n^2}{C_1 C_2}} \right]
\end{aligned}$$

or approximately

$$\gamma = \pi R \sqrt{\frac{C}{L}} = \frac{\pi}{2} \frac{C_2 - C_1}{C_r} \frac{1}{\sqrt{\left(\frac{I_A}{I_1}\right)^2 - 1}} \quad (\text{Bjerknes formula})$$

This relation is often used to evaluate either  $\gamma$  or  $R$  from an observed resonance curve if  $\omega$  is in the radio frequency range.

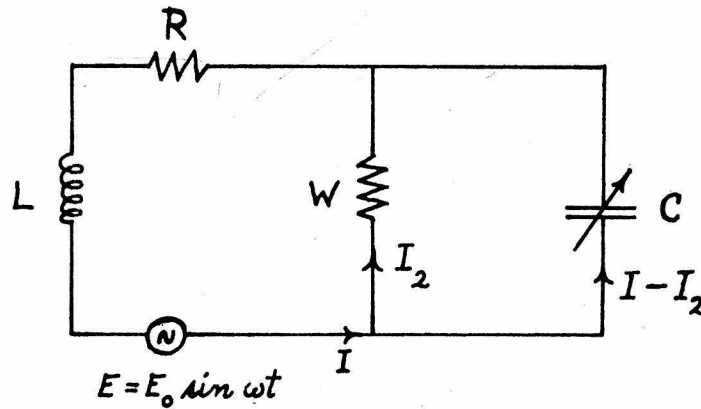


Fig. 2.2 - 1

### Section 2.2 Another resonance circuit

Let us now consider the circuit of Fig. 2.2 - 1. We have the differential equations

$$L \frac{d^2 I}{dt^2} + R \frac{dI}{dt} + \frac{I - I_2}{C} = \frac{dE}{dt} = E_0 \omega \cos \omega t$$

$$L \frac{dI}{dt} + RI + WI_2 = E_0 \sin \omega t$$

$$I - I_2 = CW \frac{dI_2}{dt}$$

whence

$$\frac{d^2 I}{dt^2} + \left( \frac{R}{L} + \frac{1}{CW} \right) \frac{dI}{dt} + \frac{1}{LC} \left( 1 + \frac{R}{W} \right) I = \frac{1}{L} \frac{dE}{dt} + \frac{E}{LCW}$$

Or, by defining  $\frac{1}{LCW} = \cot \varphi$ , this can be written

$$\frac{d^2 I}{dt^2} + \left( \frac{R}{L} + \frac{1}{CW} \right) \frac{dI}{dt} + \frac{1}{LC} \left( 1 + \frac{R}{W} \right) I = \frac{E_0 \omega}{L \sin \varphi} \sin(\omega t + \varphi)$$

The steady state solution of this equation is

$$I = \frac{E_0 \omega \sqrt{1 + \frac{1}{W^2 C^2 \omega^2}}}{L \sqrt{\left[ \frac{1}{LC} \left( 1 + \frac{R}{W} \right) - \omega^2 \right]^2 + \frac{\omega^2}{L^2} \left[ R + \frac{L}{CW} \right]^2}} \sin \left[ \omega t + \varphi - \tan^{-1} \frac{R + \frac{L}{CW}}{\frac{1}{C\omega} \left( 1 + \frac{R}{W} \right) - L\omega} \right]$$

whence the resonance capacity is

$$C_R = \frac{1}{2L\omega^2} \left( 1 + \frac{2R}{W} \right) \left[ 1 + \sqrt{1 + 4 \left( \frac{L\omega}{2R + W} \right)^2} \right]$$

The natural frequency is given by

$$\nu_0 = \frac{\omega_0}{2\pi} = \frac{1}{2\pi\sqrt{LC}} \sqrt{1 - \frac{LC}{4} \left( \frac{R}{L} - \frac{1}{CW} \right)^2}$$

The logarithmic damping decrement is

$$\gamma = \frac{1}{\sqrt{1 - \frac{LC}{4} \left( \frac{R}{L} - \frac{1}{CW} \right)^2}} \cdot \pi R \left( \sqrt{\frac{C}{L}} + \frac{1}{RW\sqrt{\frac{C}{L}}} \right)$$

In the present work the first factor differs from unity by about 0.01%.

Hence we can write

$$\gamma = \pi R \sqrt{\frac{C}{L}} + \frac{\pi}{W\sqrt{\frac{C}{L}}}$$

The value of the resonance current is approximately

$$I_r = \frac{E_o}{R + \frac{L}{WC_r}}$$

### Section 2.3 Expression for resistance in terms of observables

Let us now investigate the following procedure. Let  $W$  be an electrolytic resistance. We may fill a test condenser with distilled water and observe  $I^2$  as a function of  $C$ , varying  $C$  in the neighborhood of  $C_r$ , the resonance capacity. We plot this resonance curve and determine  $\gamma_{\infty}$  for the circuit. Next we fill the test condenser with an electrolytic solution and again experimentally determine the logarithmic damping decrement which we may now call  $\gamma_w$ . Using the above relations we shall have

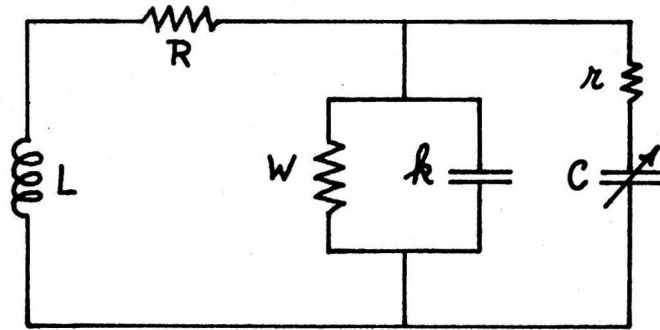
$$W = \pi \sqrt{\frac{L}{C_r}} \frac{1}{\gamma_w - \gamma_{\infty}}$$

The cell constant being known, we can calculate the specific conductivity of the solution at the frequency  $\frac{\omega}{2\pi}$  .

#### Section 2.4 Applicability of circuit diagrams

It may be worth while at this stage of our development of the experimental method used to emphasize that any radio frequency apparatus can be represented only approximately by any circuit diagram, and that its behavior can be predicted only approximately by the mathematical expressions derived in terms of such a diagram using alternating current circuit theory. It is necessary for the careful worker using radio frequency apparatus to consider not only several circuit diagrams in relation to a particular apparatus, but also to consider several variations of the apparatus itself in order to be convinced that the mathematical formulae adequately represent experimental conditions and that results obtained are independent of the apparatus used. However, for the purpose of discussion little would be gained by a complete report of such multitudinous variations; on the contrary much would be lost, for the needle would be buried in a stack of minutiae.

An example of our policy of concentrating the reader's attention on the needle is furnished by the expression for  $W$  in Section 2.3 derived in terms of the circuit diagram of Figure 2.2 - 1. Since  $W$  is an electrolytic resistance, the following diagram undoubtedly approximates closer to reality.



However, a consideration of this more complicated diagram leads to the conclusion that the formula for  $W$  in Section 2.3 is adequate. Indeed, in order for the correction terms to affect our result by 1%, it would be necessary to assume that the dielectric constant for the solution differs from the dielectric constant of distilled water by 100,000 %.

Section 2.5 A circuit used extensively

Let us now consider the circuit of Fig. 2.5 - 1.

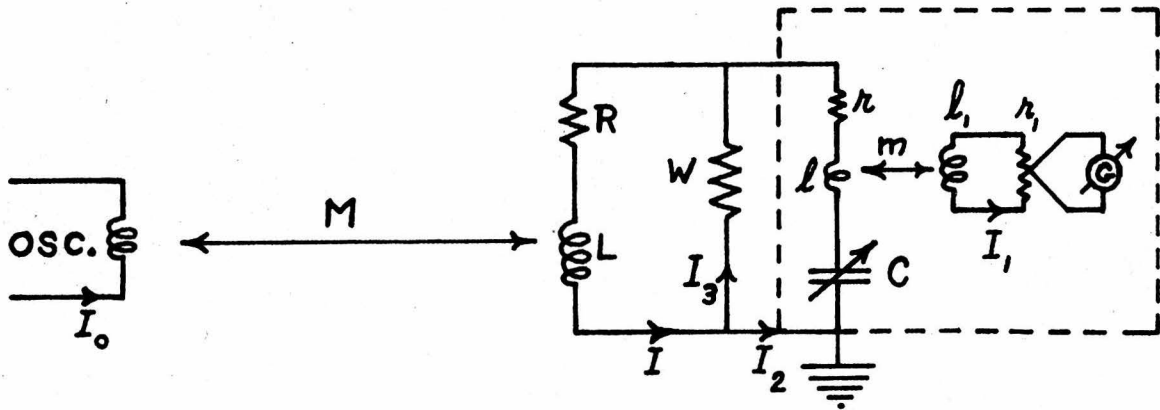


Fig. 2.5 - 1

For this case it is convenient to use complex algebra to determine the steady state relationships of the various currents. We can write

$$I = I_2 + I_3$$

$$I(R + iL\omega) + I_3 W + iM\omega I_0 = 0$$

$$-I_3 W + I_2 \left( r + i l \omega - \frac{i}{C\omega} \right) + I_1 i m \omega = 0$$

$$I_1 (r_1 + i l_1 \omega) + i m \omega I_2 = 0$$

Using the abbreviations

$$X = L\omega + l\omega - \frac{1}{C\omega}$$

$$a_r = \frac{m^2 \omega^2}{X_1^2} r_1$$

$$x = l\omega - \frac{1}{C\omega}$$

$$X_1^2 = r_1^2 + l_1^2 \omega^2$$

$$a_l = \frac{m^2 \omega^2}{X_1^2} l_1 \omega$$

and neglecting  $\frac{r}{W}$  and  $\frac{R}{W}$  compared with unity, we find

$$\left( \frac{I_0}{I_1} \right)^2 = \frac{1}{m^2 M^2 \omega^4} \left\{ \left[ m^2 \omega^2 + r_1 \frac{L^2 \omega^2}{W} - \left( l_1 \omega + r_1 \frac{L\omega}{W} \right) X \right]^2 + \left[ l_1 \omega \frac{L^2 \omega^2}{W} + \frac{m^2 \omega^2 L\omega}{W} + \left( r_1 - l_1 \omega \frac{L\omega}{W} \right) X \right]^2 \right\}$$

The resonance condition observed (i.e. the condition for maximum

$I_1 = I_{1r}$ ) is for

$$X = X_r = L\omega + l\omega - \frac{1}{C\omega} = \frac{m^2 \omega^2 l_1 \omega \left( 1 - \frac{2r_1 L}{W l_1} + \frac{L^2 \omega^2}{W^2} \right) - \frac{L^3 \omega^3}{W^2} (r_1^2 - l_1^2 \omega^2)}{X_1^2 \left( 1 + \frac{L^2 \omega^2}{W^2} \right)}$$

We have

$$\left(\frac{I_{1r}}{I_1}\right)^2 = \frac{\left[m^2\omega^2 + \kappa_1 \frac{L^2\omega^2}{W} - \left(l_1\omega + \kappa_1 \frac{L\omega}{W}\right)X\right]^2 + \left[m^2\omega^2 \frac{L\omega}{W} + l_1\omega \frac{L^2\omega^2}{W} + \left(\kappa_1 - l_1\omega \frac{L\omega}{W}\right)X\right]^2}{\left[m^2\omega^2 + \kappa_1 \frac{L^2\omega^2}{W} - \left(l_1\omega + \kappa_1 \frac{L\omega}{W}\right)X_{r_1}\right]^2 + \left[m^2\omega^2 \frac{L\omega}{W} + l_1\omega \frac{L^2\omega^2}{W} + \left(\kappa_1 - l_1\omega \frac{L\omega}{W}\right)X_{r_1}\right]^2}$$

We also derive that

$$\left(\frac{I_0}{I}\right)^2 = \frac{1}{M^2\omega^2} \left\{ \frac{\left[Wa_{r_1} + L\omega(X - L\omega - a_e)\right]^2 + \left[L\omega(W + a_{r_1}) - W(X - L\omega - a_e)\right]^2}{(W + a_{r_1})^2 + (X - L\omega - a_e)^2} \right\}$$

and

$$\left(\frac{I}{I_1}\right)^2 = \frac{1}{m^2\omega^2 W^2} \left\{ \left[l_1\omega W + \left(l\omega - \frac{1}{C\omega}\right)\kappa_1\right]^2 + \left[m^2\omega^2 + \kappa_1 W - l_1\omega \left(l\omega - \frac{1}{C\omega}\right)\right]^2 \right\}$$

For the present work the significant terms for  $\left(\frac{I}{I_1}\right)^2$  are as follows:

$$\left(\frac{I}{I_1}\right)^2 = \frac{X_1^2}{m^2\omega^2} \left(1 + \frac{1}{W^2 C^2 \omega^2}\right) + \frac{2\kappa_1}{W}$$

For a nearly symmetrical resonance curve, we may introduce the width of the curve by putting

$$C = C_r \left(1 \mp \frac{\Delta C}{2C_r}\right) \equiv C_r (1 \mp \epsilon) \quad \text{where } \mp \text{ refers to } \begin{cases} \text{left} \\ \text{right} \end{cases}$$

side of the curve.

Then

$$\frac{1}{C^2} = \frac{1}{C_r^2} (1 \pm 2\epsilon + 3\epsilon^2)$$

Hence, making obvious abbreviations,

$$\left(\frac{I}{I_1}\right)^2 = A + B(1 \pm 2\epsilon + 3\epsilon^2) \quad ; \quad \left(\frac{I_n}{I_{1n}}\right)^2 = A + B$$

Then, setting  $y = \frac{I_n}{I}$  and  $y_1 = \frac{I_{1n}}{I_1}$  we have

$$\frac{y^2}{y_1^2} = 1 \mp \alpha \Delta C + \beta \Delta C^2 .$$

The average value of  $y^2/y_1^2$  is  $\frac{1}{2}$  the sum of

$$1 - \alpha \Delta C + \beta \Delta C^2 \quad \text{and} \quad 1 + \alpha \Delta C + \beta \Delta C^2 \quad \text{or}$$

$$\frac{y^2}{y_1^2} = 1 + \beta \Delta C^2 \quad \text{when averaged over the resonance curve.}$$

Whence we obtain 
$$\frac{y^2 - 1}{\Delta C^2} = \frac{y_1^2 - 1}{\Delta C^2} + \beta y_1^2$$

Again we abbreviate, setting  $\frac{1}{\eta^2} = \frac{y^2 - 1}{\Delta C^2}$ ,  $\frac{1}{\eta_1^2} = \frac{y_1^2 - 1}{\Delta C^2}$ ,  $\frac{100}{\varphi} = y_1^2$

The significance of  $\eta$ ,  $\eta_1$ , and  $\varphi$  is then as follows. The logarithmic decrement of the circuit of Fig. 2.2 - 1 is  $\gamma = \frac{\pi}{2C} \eta$

The observed curve however yields  $\gamma_1 = \frac{\pi}{2C} \eta_1$  since we have plotted

$f I_1^2 = \varphi$  against  $C$ , not  $f I^2$  against  $C$ . The procedure is then

to calculate from the observed resonance curve corresponding values of

$\frac{1}{\eta_1^2}$  and  $\frac{100}{\varphi}$ ; next to plot  $\frac{1}{\eta_1^2}$  vs.  $\frac{100}{\varphi}$ . The value of  $\frac{1}{\eta_1^2}$  is then the ordinate corresponding to  $\frac{100}{\varphi} = 1$  plus the absolute value

of the slope of the resultant straight line, the equation for which we have seen to be

$$\frac{1}{\eta^2} = \frac{1}{\eta_1^2} + \beta \frac{100}{\varphi}$$

Having determined  $\eta$  in this manner, we have

$$W = \pi \sqrt{\frac{L}{C}} \frac{1}{\gamma_w - \gamma_{\infty}} = \pi \sqrt{\frac{L}{C}} \frac{2C}{\pi} \frac{1}{\eta_w - \eta_{\infty}} = \frac{1}{\pi \nu (\eta_w - \eta_{\infty})} = \frac{\lambda}{\pi \nu \Delta \eta}$$

Examples are given in section 4.1.

#### Section 2.6 Other circuits tested

Two circuits were considered mathematically and tested experimentally in addition to that of Figure 2.5 - 1. Essentially the same conclusions were reached as to the proper procedure to obtain the invariant  $\Delta \eta$  corresponding to a given  $W$ . Figure 2.6 - 1 shows one of these circuits, which is objectionable because of the somewhat large "background" deflection of the galvanometer. Figure 2.6 - 2 shows the other circuit; it is objectionable because of the excessively large value of  $\eta_{\infty}$  it yields, and the relatively large value of  $M$  it demands.

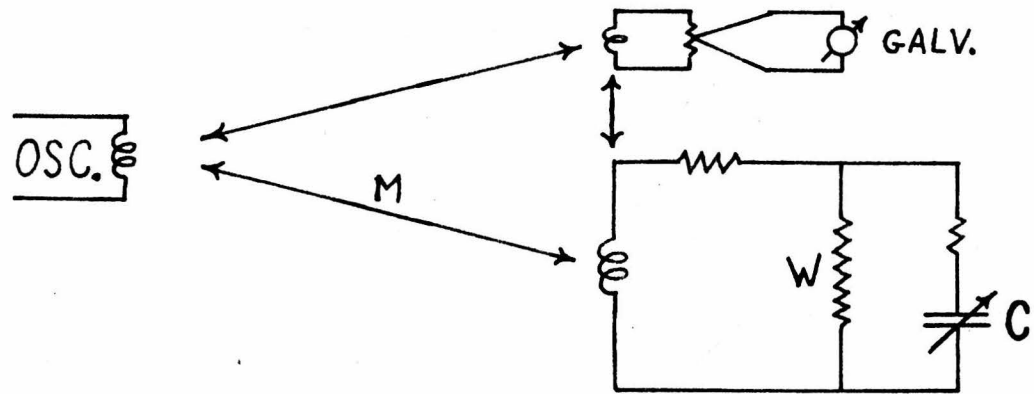


Figure 2.6 - 1

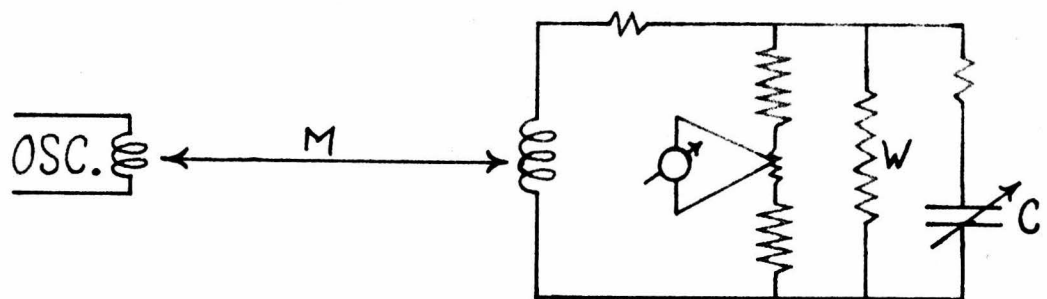


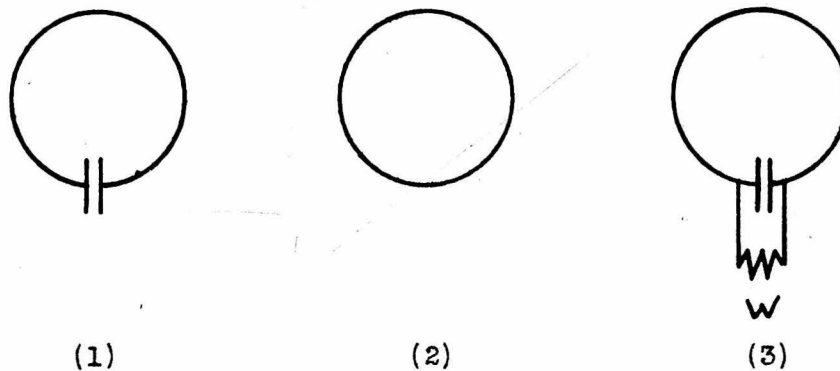
Figure 2.6 - 2

### Section 2.7 Radiation resistance

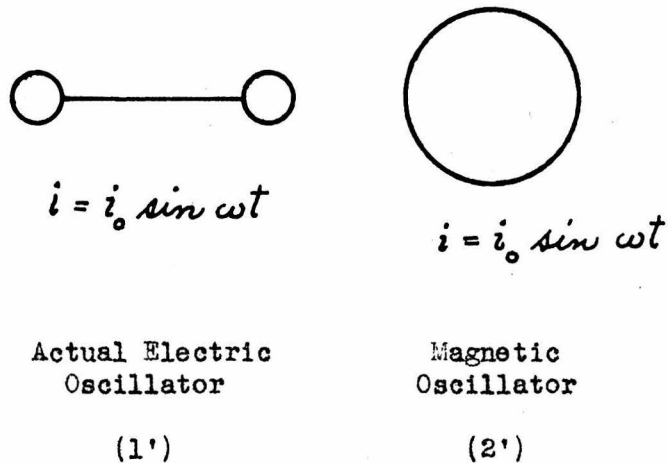
The effect of a change in the radiation resistance of the circuit shown in Figure 2.2 - 1 due to a change in  $W$  and  $\lambda$  may introduce an appreciable error into the value of  $W$  determined as above. The circuit may be expected to radiate more energy for the same current and wave length when  $W = 10^7$  ohms than when  $W = 10^4$  ohms, since for a

constant induced electromotive force the fraction of the total power dissipated in the form of heat increases as  $W$  decreases. This can be illustrated in the following way.

Let us consider the three circuits 1, 2, 3 below and the



analogous circuits (1') and (2') for which we quote\* the average power



radiated respectively:

\* Page and Adams: Principles of Electricity, p. 588, 1931 edition.

$$\bar{P}_{RE} = \frac{4\pi^2 c i_0^2 l^2}{3\lambda^2} \quad (\text{e.m.u.}); \quad \bar{P}_{RM} = \frac{4\pi^3 i_0^2 A^2}{3c\lambda^4} \quad (\text{h.l.u.})$$

Whence, for the same  $i_0$  and  $\lambda$ ,

$$\frac{\text{Radiation from Magnetic Oscillator}}{\text{Radiation from Electric Oscillator}} = \frac{\bar{P}_{RM}}{\bar{P}_{RE}} = \left( \frac{2\pi A}{\lambda l} \right)^2.$$

Since the linear dimensions are small compared with the wave length, a magnetic oscillator is inefficient compared with an electric oscillator as a source of electromagnetic waves. Our circuit (3) considered as a radiator is intermediate between circuits (1) and (2) and hence between circuits (1') and (2'), and approaches the characteristics of (2') as  $W$  decreases. We conclude that the radiation resistance of circuit (3) decreases as  $W$  decreases.

Let the radiation resistance,  $r$ , be a function of  $W$  and  $\lambda$ . We expand the function in terms of the dimensionless ratio  $\frac{2\pi\nu L}{\lambda W}$  which is of the order  $10^{-3}$ , and retain the first two terms. Thus

$$r = r_0 - r_1 \frac{2\pi\nu L}{\lambda W} \quad \text{where } r_1 \text{ is positive according to the}$$

above considerations. Then instead of having  $\gamma_w - \gamma_\infty = \frac{\pi}{W\sqrt{\frac{c}{L}}}$

$$\text{we shall have } \gamma_w - \gamma_\infty = \frac{\pi}{W\sqrt{\frac{c}{L}}} - r_1 \frac{2\pi\nu L}{\lambda W} = \frac{\pi}{2c} \Delta\eta$$

whence

$$\frac{1}{W} = \frac{\pi\nu\Delta\eta}{\lambda} + \left( \frac{\lambda}{2\pi\nu L} \right)^2 r_1 \frac{2\pi\nu L}{\lambda W} = \frac{\pi\nu\Delta\eta}{\lambda} + r_1 \frac{\lambda}{2\pi\nu L} \cdot \frac{1}{W}$$

We now distinguish between the true high frequency resistance,  $W$ , and the erroneous value  $\frac{\lambda}{\pi \nu \Delta \eta}$ , calling the latter  $W'$ . Thus we can write

$$\frac{1}{W} = \frac{1}{W'} + \kappa, \frac{\lambda}{2\pi \nu L} \frac{1}{W} \quad \text{or} \quad \frac{W}{W'} = 1 - \frac{\kappa, \lambda}{2\pi \nu L} .$$

Hence for a given circuit and wave length, we may expect to find the measured  $W'$  larger than (and perhaps proportional to\*) the true value  $W$ . By determining  $W'$  for carbon resistors, and identifying their low frequency resistance with  $W$ , we can correct our observations on electrolytes to eliminate this effect.\*\*

#### Section 2.8 Temperature correction

Solutions were prepared by weighing the salts and measuring the volume of the solutions formed. The equivalent conductivity of each solution at low frequencies was then taken from the International Critical Tables for temperatures of 18° C and 25° C. The quantity

$$\alpha = \frac{\Lambda_{25} - \Lambda_{18}}{7 \Lambda_{18}} \quad \text{was then calculated for each solution. In}$$

order to reduce results,  $\Lambda_t$ , from room temperature to 18° C. the

\* Figure 4.1 - 6 indicates that this is true for the range of  $W$  of interest.

\*\* Section 4.3, sources of error.

following expression was then used:  $\Lambda_{18} = \frac{\Lambda_t}{1 + \alpha(t-18)}$ .  $\alpha$  is of the order 2.4% per degree centigrade.

### Section 2.9 Test cell constants

Cell constants  $k = W \sigma$  were determined by measuring  $W$  at 500 and 1000 cycles per second by two different bridge methods using solutions prepared as above. The error in  $k$  is less than 1%.

### Section 2.10 Adjustment of circuit constants

The various circuit constants must be adjusted to satisfy the following conditions in order to achieve satisfactory accuracy (or, in some cases, to make resonance curves observable at all).

- (1) The product  $LC$  is determined by the frequency.
- (2)  $R\sqrt{\frac{C}{L}}$  must be large enough to permit determination of  $\eta_{\infty}$  with satisfactory accuracy, but at the same time small enough to permit  $\eta_w$  and  $\Delta\eta$  to be satisfactorily large compared with  $\eta_{\infty}$ .
- (3)  $W\frac{C}{L}$  must be large enough to permit observation of the corresponding resonance curve with sufficient accuracy, but  $W\sqrt{\frac{C}{L}}$  must simultaneously be small enough to permit  $\eta_w$  and  $\Delta\eta$  to be satisfactorily large compared with  $\eta_{\infty}$  and also to permit use of the same condenser calibration at all frequencies.

- (4)  $\left(\frac{L\omega}{W}\right)^2$  must be small compared with unity in order that the resonant capacity for  $W \neq \infty$  be satisfactorily near the resonant capacity for  $W \sim \infty$ .

These requirements can be satisfied if  $W$  is in the interval 8000 to 16000 ohms for  $\lambda$  between 15 and 45 meters and necessitate the use of more than one test cell to cover the range of concentrations studied, for the specific conductivity changes over this range by a factor of 1270.

Section 2.11 Calculation of  $\Lambda_\omega$  from observables

To determine the quantity  $\frac{\Lambda_\omega - \Lambda_0}{\Lambda_0}$  at 18° C., in which form we have expressed the results, the procedure is as follows:

- (1) Observe a resonance curve (galvanometer deflections corresponding to condenser reading in divisions) with a cell filled with distilled water.
- (2) Observe a resonance curve with the same cell filled with a solution of appropriate concentration.
- (3) Multiply all galvanometer deflections by a factor of such size as to place the peak value at 100 cm., and plot these values of  $\varphi$  against the condenser readings in divisions.
- (4) Determine the widths of these curves (in  $\mu\mu\text{fd.}$ ) at appropriate values of  $\varphi$ . These widths have been called  $\Delta C$ .

- (5) Calculate the quantities  $\frac{1}{\eta^2} = \frac{\frac{100}{\varphi} - 1}{\Delta C^2}$  and  $\frac{100}{\varphi}$ . Plot the former as ordinates vs. the latter. If a straight line can not be drawn justifiably through these points, readjust the circuit constants - that is, redesign the apparatus.
- (6) Record the ordinate of this straight line corresponding to  $\frac{100}{\varphi} = 1$  and its slope. Take the sum, intercept + |slope|, which is  $\frac{1}{\eta^2}$ . Calculate  $\eta_{\infty}$  from curve (1),  $\eta_w$  from curve (2).
- (7) Calculate  $\Lambda_t = \frac{10^{-6} \pi v k \Delta \eta}{\gamma^* \lambda}$
- (8) Correct this value to  $\Lambda$  at 18° C.
- (9) Apply the correction for radiation resistance, obtaining  $\Lambda_{\omega}$ .
- (10) Form  $\frac{\Lambda_{\omega} - \Lambda_0}{\Lambda_0} = \frac{\sigma_{\omega} - \sigma_0}{\sigma_0}$ .

#### Section 2.12 An alternative method

An alternative method, which may already have occurred to the reader, might be based on the observation of the current at resonance only, instead of observation of the entire resonance curve. This procedure was actually followed at the wave length of 4.04 meters only. Although it permits a great saving of time, this method can not be so accurate or even so reliable as that involving the use of the entire

resonance curve. Indeed, this alternative method, if it had been used before the other procedure had given knowledge of various important properties of the apparatus, would have led to large errors perhaps as great as 50%.

We proceed to discuss the manner in which the results at 4.04 meters wave length only were obtained. At the end of section 2.2 we had

$$I_{\kappa} = \frac{E_0}{R + \frac{L}{WC_{\kappa}}}$$

We derive that  $W = \frac{\frac{\pi}{\gamma_{\infty}} \sqrt{\frac{L}{C}}}{\frac{I_{\kappa\infty}}{I_{\kappa W}} - 1}$  and calling the numerator

a constant, A, and writing the galvanometer deflection ratio for the current ratio we have

$$W = \frac{A}{\sqrt{\frac{\theta_{\kappa\infty}}{\theta_{\kappa W}} - 1}}$$

or abbreviating

$$W = \frac{A}{\sqrt{\frac{\theta_{\infty}}{\theta_w} - 1}}$$

By using carbon resistors, A and  $\theta_{\infty}$  can be empirically determined (for accuracy in determining  $\theta_w$  it is better to make  $\theta_{\infty}$  too large to be observed). The values of  $\theta_w$  are constant to about 1 part in a thousand. Nevertheless, in a typical experiment, the values  $A = 3980 \text{ ohms} \pm 2.5\%$  and  $\sqrt{\theta_{\infty}} = 8.992 \text{ cm.}^{\frac{1}{2}} \pm 0.8\%$  were determined. Thus it is evident that this method is less accurate than the method using the entire resonance curve.

Chapter 3. The apparatus

## Section 3.1 Oscillators

For wave lengths greater than 15 meters the oscillator circuit was of the Hartley type using one RCA 800 tube rated at 35 watts. For wave lengths less than 15 meters the oscillator was of the tuned line type using the same tube. Of several oscillators of the latter type constructed, the design which proved most satisfactory is illustrated in Fig. 3.1 - 1.

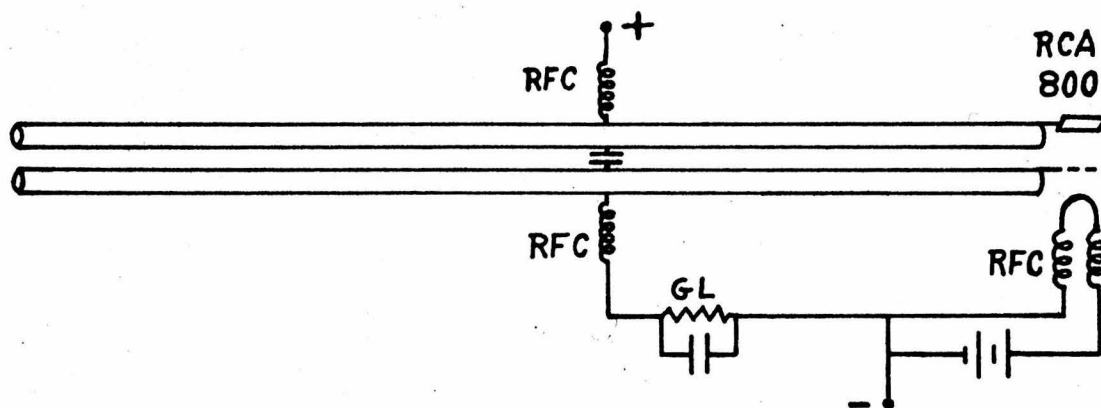


Fig. 3.1 - 1

Filament and plate voltages were furnished by storage batteries.

## Section 3.2 Resonance indicator system

The resonance indicator consisted of a vacuum thermocouple-galvanometer system. The heater resistance of the couple was approximately 1000 ohms; the couple resistance was about 15 ohms. The galvan-

ometer was of the d'Arsonval voltage sensitive type having a resistance of about 15 ohms. A light beam and scale was used. For a heater current of 0.28 milliamperes the deflection on the scale was 100 cm., hence a difference of heater current amounting to 94 microamperes could be detected. A galvanometer shunt made it possible to observe heater currents as large as 2 milliamperes.

### Section 3.3 Resonance circuit

The variable air condenser\* in the resonance circuit was contained in a cylindrical copper case (diameter 15 cm., height 9 cm.). A plate of silica supported all metal parts of the condenser. There were two coaxial rotor shafts. On one of these was mounted a single semi-circular plate, rotation thru  $180^\circ$  being effected by rotating the worm shaft 25 times, thereby producing a capacitance change of about 10  $\mu\mu$  fd. A drum on the worm shaft was divided into 200 divisions by a vernier. The least count was then 0.0002  $\mu\mu$  fd. theoretically. This drum was observed thru a telescope and rotated by means of a hard rubber shaft 1 meter long. The other rotor produced a large capacity change of as much as 800  $\mu\mu$  fd. (depending upon the number of plates used). The minimum capacitance between the stator and the rotor was less than 10  $\mu\mu$  fd. The worm was of steel; all other metal parts were of brass, phosphor bronze, or copper.

\* Please see photographs below.

The chief current path surfaces were gold plated. All sliding contacts were by-passed electrically by solder or large-surface mercury connections. The entire design was mechanically strong, calibration-stable, and electrically satisfactory for the purpose.

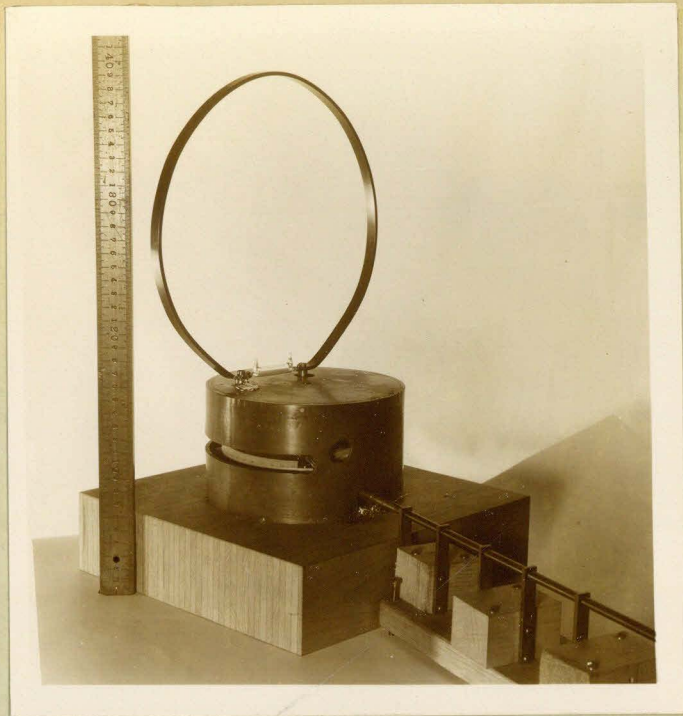
Calibration of the vernier plate was effected using the substitution method at  $\lambda = 50$  m., the substitution capacitance being of a calculable type.

The coils used were loops of heavy copper strip.

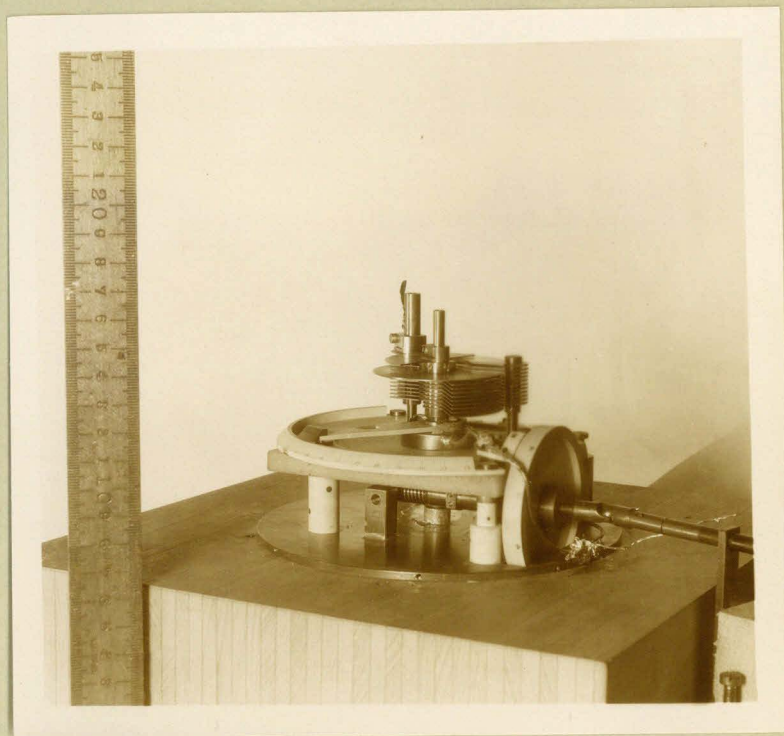
The test cells\* used were of pyrex glass with platinum electrodes. Six were necessary to cover the range of concentrations.

Wave lengths were determined using a General Radio Company precision wavemeter, type 224 L, or by using a wavemeter previously calibrated in terms of a Lecher wire system.

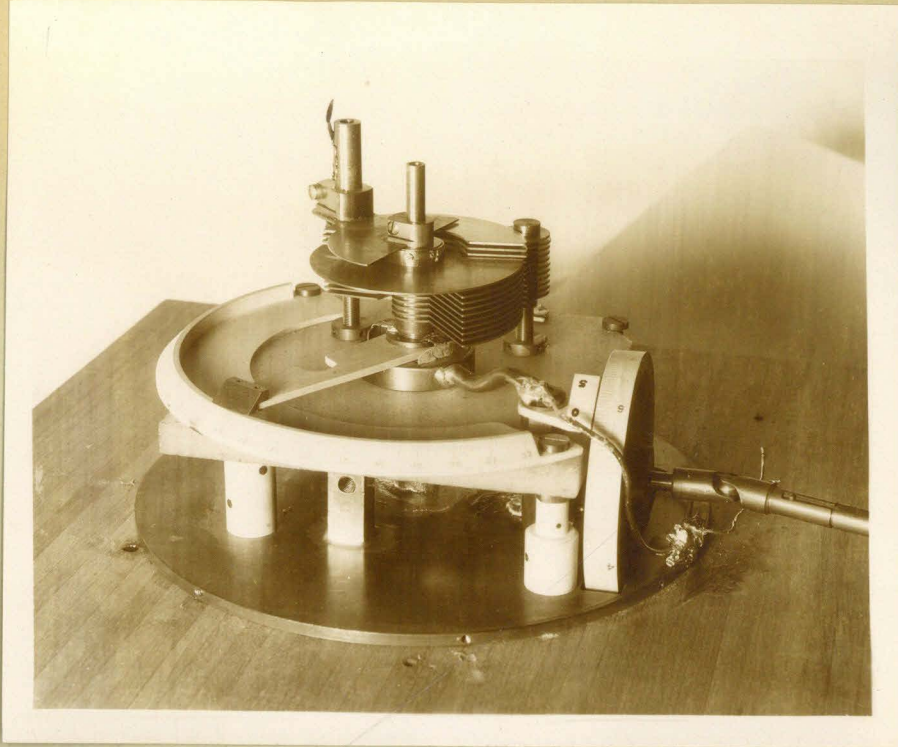
\* Please see photograph below.



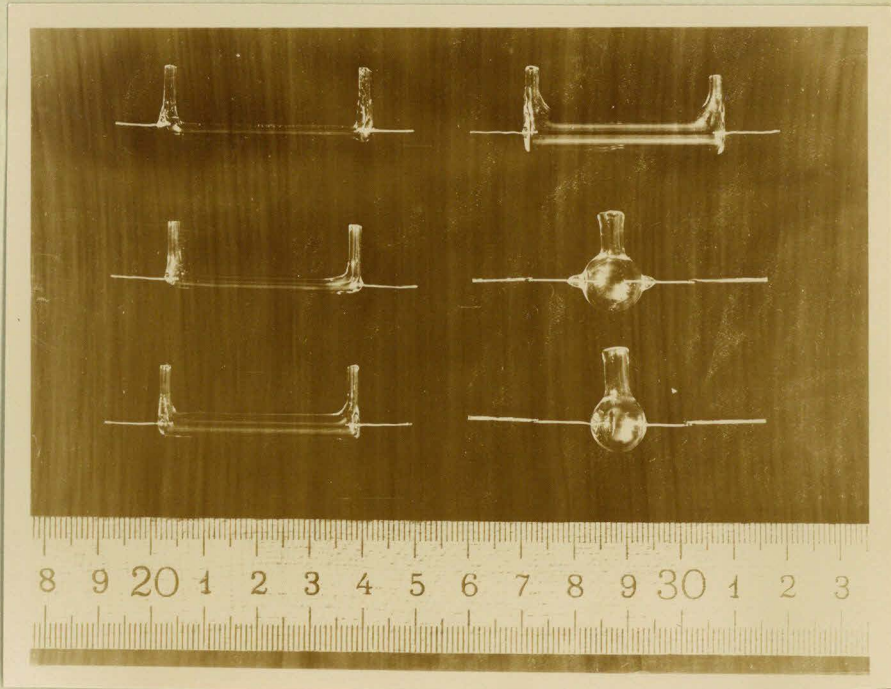
The resonance circuit used at  $\lambda = 27.4$  meters, showing the removable coil, a test cell in position, the condenser shielding case inside which the thermocouple was mounted, and the drive shaft.



The precision condenser showing the drive shaft connection to the worm driving the single rotor plate.



The precision condenser showing the two rotors separated by the shielding plate, and the adjustable stator.



The test cells used.  
 Cell constants  $k = W\sigma$  in  $\text{cm}^{-1}$   
 appear in corresponding positions.

Cell constants	
715.	16.0
210.4	3.01
55.5	0.580

#### Chapter 4. Test of the method and sources of error

##### Section 4.1 Tests of the mathematical theory of the method.

In the first place it was necessary to test the mathematical conclusions of Chapter 2 in order to establish the validity of the experimental method to the writer's satisfaction. A limited amount of evidence will now be presented which, it is hoped, will convince the reader that the method is sound. The following examples are determinations of the high frequency resistance of carbon resistors, which are chosen to illustrate a variety of points; the quality of the examples is average.

Figure 4.1 - 1 shows a variety of resonance curves. Curves 33.0 and 31.3 may be called typical for this research. Curves 102.5 and 17.6 are unusual. Curve 17.6 exhibits the undesirable characteristic of extremely small  $\eta_{\infty}$  (0.351  $\mu\mu\text{fd.}$ ), too small to be compatible with good accuracy. It is of interest to note that this curve was recorded twice, and when plotted "life size" the two sets of data points agreed with the curve to a distance of about 1 mm. - an indication of the constancy of the battery operated oscillator and of the electrical excellence of the precision condenser. Curve 102.5 exhibits a degree of flatness approaching unobservability. It was recorded for the special purpose of giving the 2000 ohm point on Figure 4.1 - 6. The curves are all quite symmetrical - greater symmetry would be evidenced,

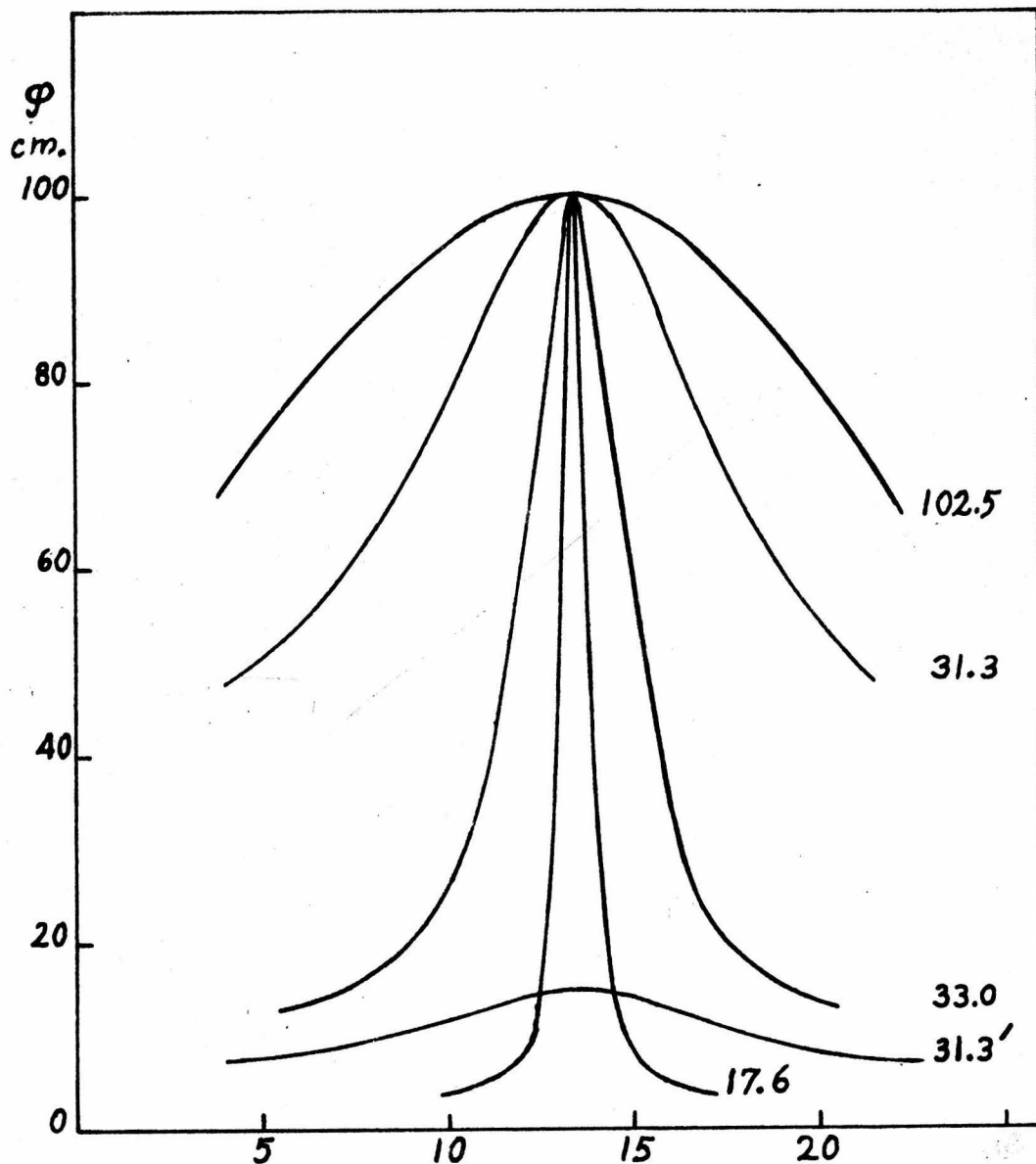


Figure 4.1-1

As abscissae are plotted revolutions of the drum (25 of which represent a rotation of  $180^\circ$  of the single plate of the precision condenser). The ordinates are obtained by multiplying observed galvanometer deflections by a factor  $f$  such that  $f = 100\text{cm}$ . The ordinates for curve 31.3 only are the observed galvanometer deflections. The widths of these curves for various  $\lambda$  and the values of  $f$  are included in Table 4.1-5a immediately below.

Data Number	$\phi$	Width ( $\mu\text{mfd.}$ )	$f$	$\lambda$ (m.)	$\eta$ ( $\mu\text{mfd.}$ )	$\Delta\eta$ ( $\mu\text{mfd.}$ )	$W$ Ohms
102.5	85	5.42	2.093	27.4	11.82	10.56	2,760.
31.3	75	3.44	6.73	27.4	4.36	2.82	10,300.
33.0	50	1.615	1.109	27.4	1.42	—	—
17.6	50	0.357	1.140	27.4	0.351	—	—

Figure 4.1-2.

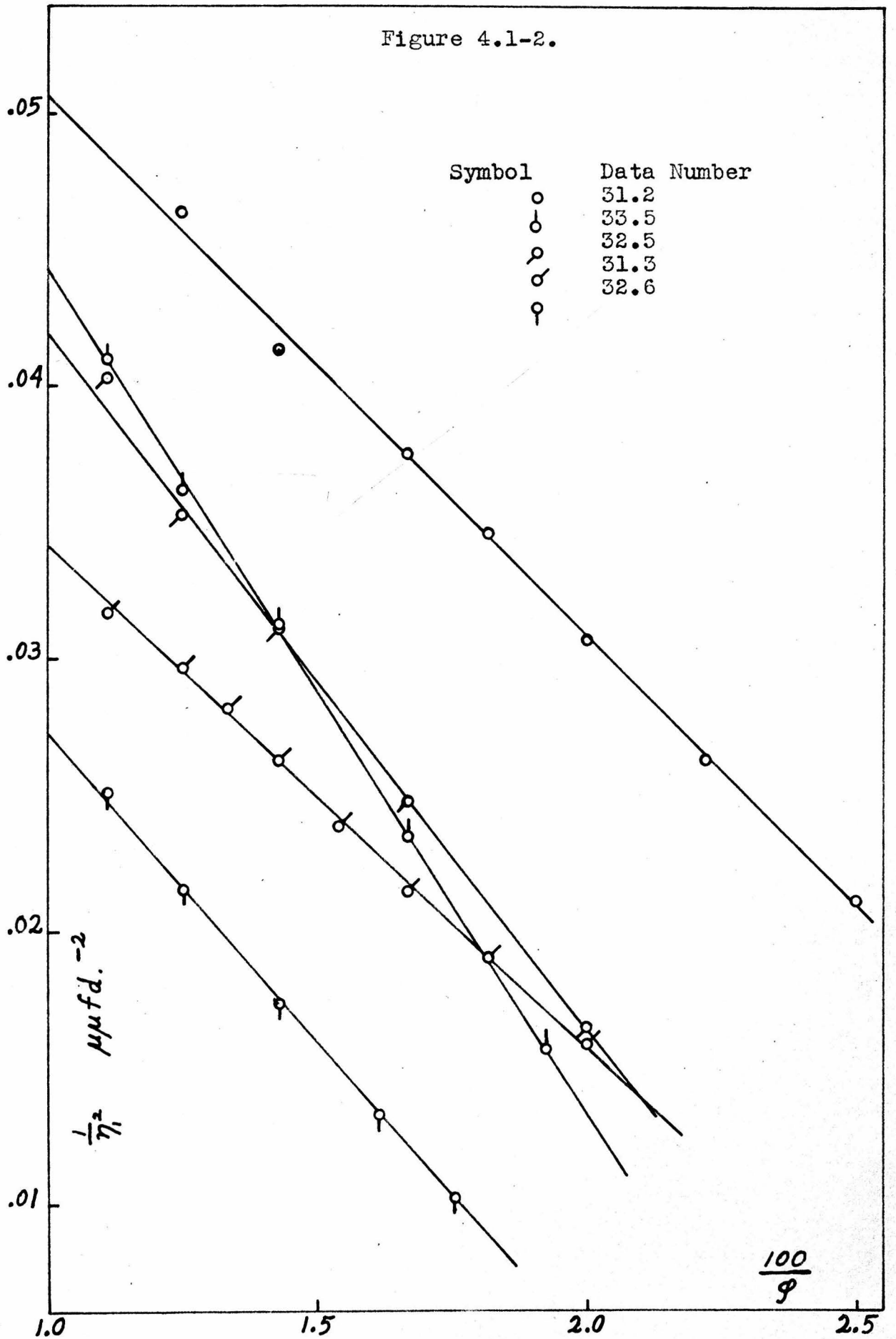


Figure 4.1-3.

Symbol	Data Number
○	31.0
◊	32.7
⊗	33.0
⊙	103.2
⊖	103.5
⊕	51.2

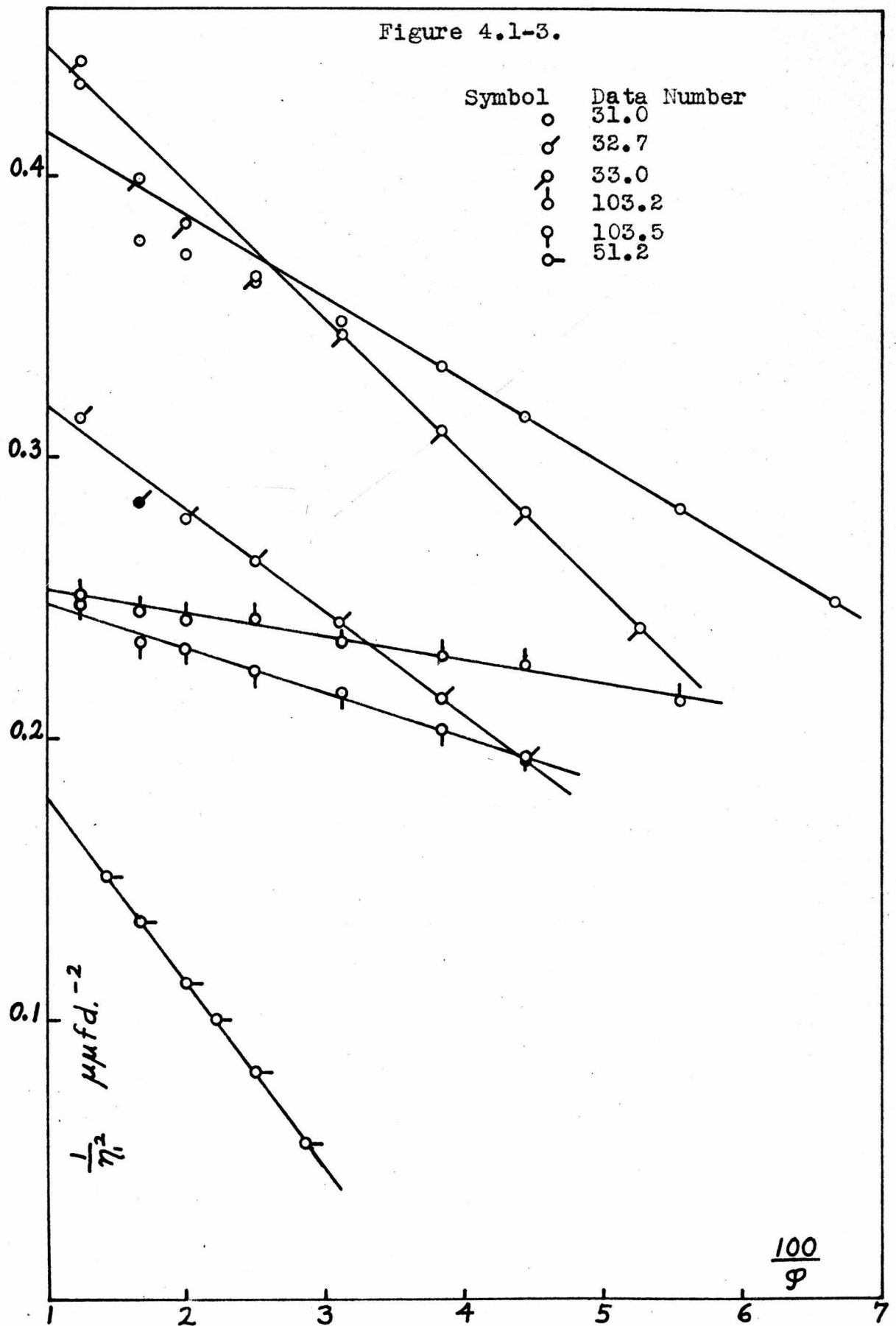
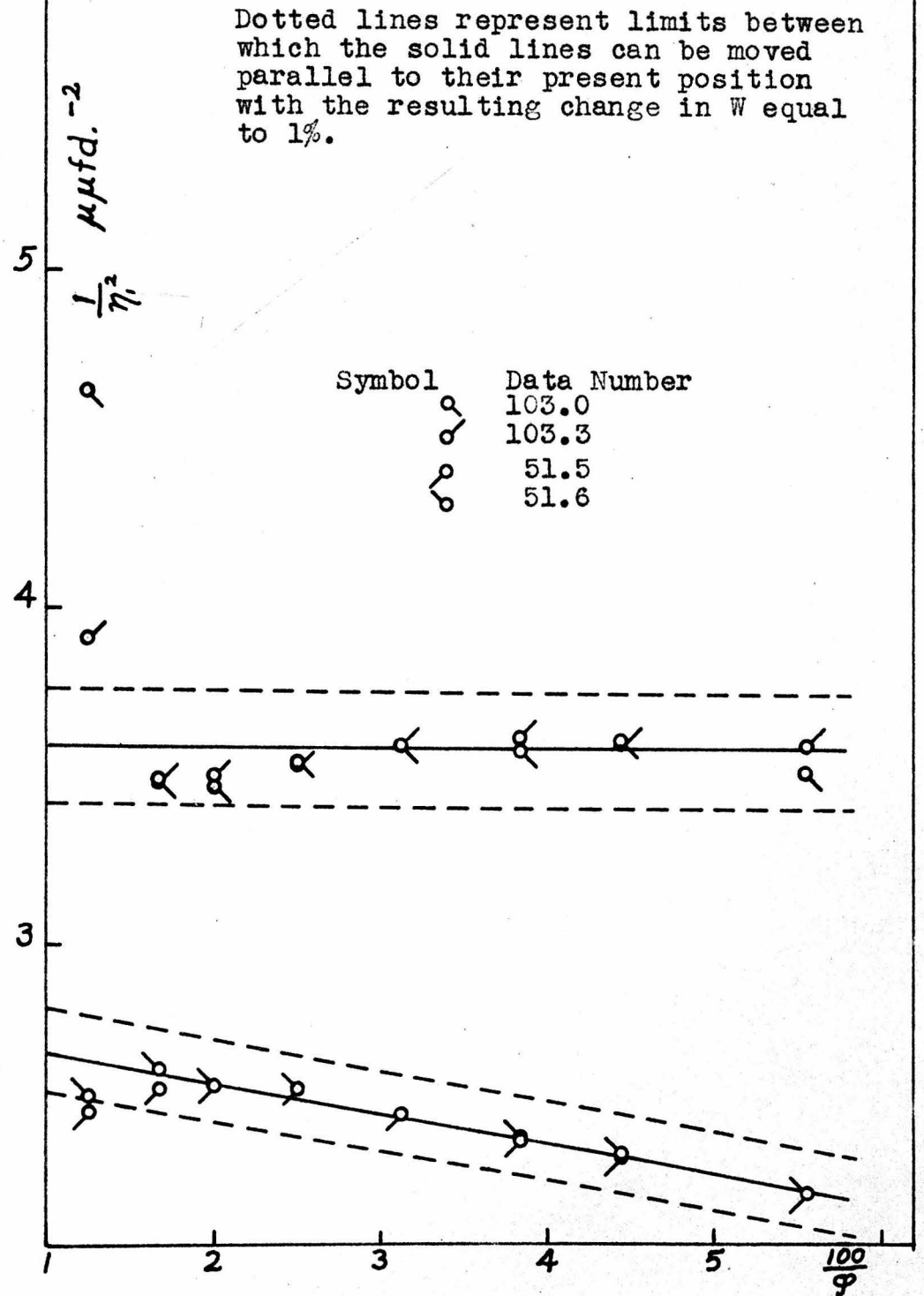


Figure 4.14



however, had they been plotted against capacity instead of drum revolutions.

Figures 4.1 - 2, 4.1 - 3, and 4.1 - 4 show the quality of the straight lines obtained by plotting  $1/\eta_1^2$  vs.  $100/\varphi$  at two wave lengths. The position of the data points in Figure 4.1 - 4 corresponding to narrow curve peaks and therefore to small values of  $\Delta C$  is partly due to observational errors in determining  $\Delta C$  and partly explicable in terms of the mathematical theory of the method. For reconsider the averaging process in which we added the following two expressions corresponding to different sides of the resonance curve:

$$\frac{y^2}{y_1^2} = 1 - \alpha \Delta C + \beta \overline{\Delta C}^2 \quad \text{and} \quad \frac{y^2}{y_1^2} = 1 + \alpha \Delta C + \beta \overline{\Delta C}^2$$

The result we wrote was

$$\frac{y^2}{y_1^2} = 1 + \beta \overline{\Delta C}^2$$

which is subject to previous approximations. It should have been  $\frac{y^2}{y_1^2} = 1 + \epsilon \Delta C + \beta \overline{\Delta C}^2 +$  (higher powers of  $\Delta C$ ) where the magnitude and sign of  $\epsilon$  is dependent on the degree of symmetry of the resonance curve and the side from which perfect symmetry is approached. Our final formula  $\frac{1}{\eta^2} = \frac{1}{\eta_1^2} + \beta \frac{100}{\varphi}$  is thus lacking in a term involving  $\frac{\epsilon}{\Delta C}$ , and for sufficiently small  $\Delta C$  the data points fall above or below the "straight line" depending on the sign of  $\epsilon$ . Fortunately it is possible to attain

good accuracy in spite of this defect as indicated by the dotted lines of Figure 4.1 - 4. The defect is usually not noticeable for larger peak values of  $\Delta C$  as shown by Figures 4.1 - 2 and 4.1 - 3. The present method of analyzing resonance curves actually works better for those curves for which the simple Bjerknes formula\* is less satisfactory.

We refer the reader now to Table 4.1 - 5b in which further information is listed concerning these examples. The data number 31.2 means that this resonance curve was the second recorded during run number 31.  $\Delta \eta = \eta_w - \eta_\infty$  is formed by using values of  $\eta$  from the same run. To form  $\Delta \eta$  31.2 we subtract  $\eta_\infty$  furnished by 31.0 from  $\eta_w$  furnished by 31.2 - thus  $3.776 - 1.537 = 2.239$ .

$f$  is the factor which is necessary to reduce all curves to the same peak value. For instance, considering data numbers 103.2 and 103.5 we notice that the actual peak galvanometer deflection observed for the latter curve was  $17.39 \div 1.246$  or 14 times greater than the resonance deflection for the former. The agreement of these two values of  $\eta_w$  to within 1% shows that the resistance of the carbon resistors (CR) was not changed due to heating within the observational uncertainty, and that the results are independent of the coupling with the oscillator. (This test was also used with electrolytic resistances with the same result.)

$\lambda$  is the wave length. The slopes and intercepts of the

\* Section 2.1

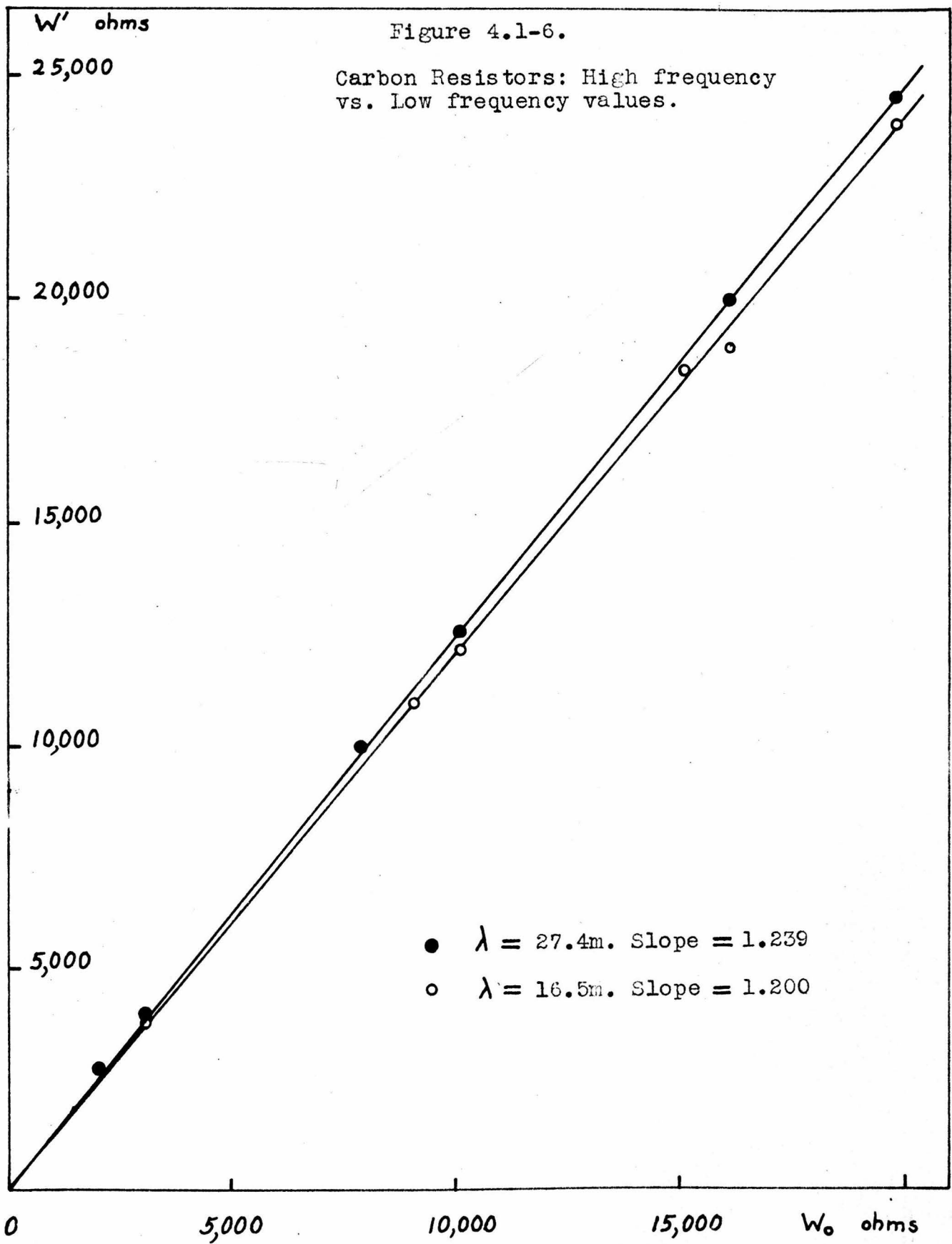
Table 4.1 - 5 b

Data Number	f	$\lambda$ m.	Slope $(\mu\mu\text{fd.})^{-2}$	Intercept $(\mu\mu\text{fd.})^{-2}$	$\eta$ $\mu\mu\text{fd.}$	$\Delta\eta$ $\mu\mu\text{fd.}$	$W_{\omega} \times 10^{-3}$ ohms	$\frac{W_{\omega}}{W_0}$	Remarks
31.2	5.40	27.4	0.0196	0.0505	3.776	2.239	13.0	1.28	CR 4
33.5	5.07	27.4	0.0308	0.0442	3.65	2.23	13.04	1.286	CR 4
32.5	4.45	27.4	0.0252	0.0416	3.87	2.195	13.27	1.307	CR 4
31.3	6.73	27.4	0.0184	0.03413	4.36	2.823	10.3	1.298	CR 3
32.6	5.25	27.4	0.0224	0.0271	4.497	2.822	10.3	1.298	CR 3
31.0	1.10	27.4	0.025	0.399	1.537	-	-	-	Cell 1.5, H <sub>2</sub>
32.7	1.112	27.4	0.0365	0.3175	1.68	-	-	-	Cell 4; H <sub>2</sub> O
33.0	1.109	27.4	0.0488	0.447	1.42	-	-	-	Cell 4; H <sub>2</sub> O
103.2	17.39	16.5	0.0078	0.251	1.966				CR 3
103.5	1.246	16.5	0.0156	0.2472	1.950	1.430	12.21	1.204	CR 3
51.2	9.7	16.5	0.0645	0.1785	2.028	1.427	12.25	1.207	CR 3
103.0	1.227	16.5	0.007	3.587	0.528	-	-	-	Nothing
103.3	1.217	16.5	0.007	3.587	0.528	-	-	-	Nothing
51.5	1.051	16.5	0.094	2.676	0.6004	-	-	-	Cell 3, H <sub>2</sub> O
51.6	1.051	16.5	0.090	2.673	0.6013	-	-	-	Cell 3, H <sub>2</sub> O

rectified resonance curves are recorded.  $W_{\omega}$  is calculated using the relation  $W_{\omega} = \frac{\lambda}{\pi \nu \Delta \eta}$ .  $W_0$  is the value of the various carbon resistors, as determined with bridge circuits using direct current and 500 and 1000 cycles per second alternating current.

We point out several examples where changes in slope are compensated by changes in intercept so that the sum, slope plus intercept, remains constant and hence  $\eta_{\infty}$ ,  $\eta_w$ ,  $\Delta \eta$  and  $W_{\omega}$  also remain constant. Compare 51.2 with 103.2 and 103.5 for  $\eta_w$  and 51.5 and 51.6 with 103.0 and 103.3 for the corresponding values of  $\eta_{\infty}$ . The reader will be able to find other examples in this table.

The first five values of  $W_{\omega} \div W_0$  for two different carbon resistors show the constancy of this ratio which is used as a multiplicative factor to correct the observed  $\Lambda_{\omega} \div \Lambda_0$  of electrolytic solutions for the radiation resistance effect. This ratio changes with the wave length but evidently  $\frac{W_0}{W_{\omega}} - 1$  is not proportional thereto; hence  $r_1$  of section 2.6 is a function of  $\lambda$ . The data plotted in Figure 4.1 - 6 indicate the constancy of this ratio for a rather extended range of  $W_0$ . The observational uncertainty is relatively large for the smaller values of  $W_0$ , and so the straight lines seem justified. We do not wish to insist, of course, that  $W_{\omega}$  is proportional to  $W_0$  for  $0 < W_0 < 5000$  ohms - only that such is the case for  $10,000$  ohms  $< W_0 < 15,000$  ohms. Changes in circuit constants affect this ratio, and rather drastic changes were purposely

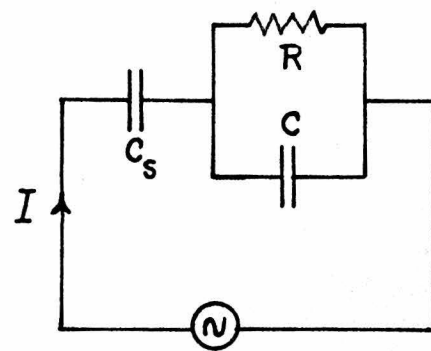
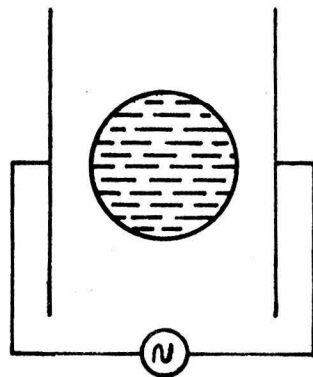


made from time to time, but no further information concerning this ratio was ascertained.

#### Section 4.2 The selective heating effect.

The selective heating effect\* is a well-established phenomenon of great importance in the field of electrotherapy. Depending upon the experimental set-up and procedure, results vary somewhat, but the essential fact is that if an electrolytic solution be subjected to a high frequency field there is observed maximum heating of the solution for that specific conductivity  $\sigma = \sigma_{max}$ . such that approximately  $\sigma_{max} = \frac{\epsilon \nu}{2}$  where  $\epsilon$  is the dielectric constant of the solution and  $\nu$  is the frequency. This effect, according to a number of workers, is explicable in terms of the geometry of the set-up used to study it.

This view can be illustrated simply as follows. Consider a volume of solution placed in a high frequency field as shown below.



$$V = V_0 \sin \omega t$$

\* Please see bibliography, part II.

The circuit diagram may be chosen as shown. Then\*

$$I = \frac{V_0}{\frac{1}{iC_s \omega} + \frac{1}{\frac{1}{R} + iC\omega}} \quad \text{and the power dissipated in}$$

the solution is

$$P = V_0^2 \frac{R}{R^2 \left(1 + \frac{C}{C_s}\right)^2 + \frac{1}{C_s^2 \omega^2}} = I^2 \frac{R}{1 + R^2 C^2 \omega^2}$$

If the voltage be held constant, the maximum power loss occurs for  $R = 1/(C + C_s)\omega$ ; if the current be held constant, the maximum loss occurs for  $R = 1/C\omega$ . Writing  $R = d/\sigma A$  and  $C = \epsilon A/4\pi d$  we have  $RC = \epsilon/4\pi\sigma$  and for constant current  $RC = 1/2\pi\nu = \epsilon/4\pi\sigma_{\max}$  or  $\sigma_{\max} = \frac{\epsilon\nu}{2}$ . The refinements and variations of this analysis will readily occur to the reader. (Certainly it needs refinement, but the original statement will not be altered thereby.) Thus it is the generally accepted view of observers of this effect that the selective heating is an apparatus effect, and is well understood without assuming that the conductivity of electrolytes is a function of frequency.

We assert that the selective heating effect did not influence the results of this research. In the first place, the formulae developed in Chapter 2 have been shown theoretically and experimentally

\* McLennan and Burton, Canadian J. Res., 5, 550 (1931)

to be adequate (in particular please recall Sections 2.4 and 2.6). In the second place, during the process of recording the resonance curves the solutions did not exhibit an appreciable rise in temperature above room temperature. As will be shown later, fractional increases in conductivity of the solutions of the order of 15% have been observed. To explain this as due to a rise in temperature of 6° C is impossible. Furthermore, the same value of conductivity was calculated for cases in which peak galvanometer deflections were of the order of 30 times greater (using galvanometer shunt) than those normally used. If normally the temperature were raised 6° C, then in the latter experiments the solutions should have boiled.

#### Section 4.3 Other sources of error.

For electrolytes the skin effect is negligible. For the carbon resistors used it is negligible because of their construction. However, considering a solid cylinder of carbon instead of the actual cylindrical surface coating of carbon, and substituting into Rayleigh's formula\*

$$* \quad \frac{R'}{R} - 1 = \frac{1}{12} \left( \frac{\omega l \mu}{R} \right)^2 - \frac{1}{180} \left( \frac{\omega l \mu}{R} \right)^4 + \dots$$

provided  $\left( \frac{\omega l \mu}{R} \right)^2 < 1$ , where

$R'$  = high frequency resistance

$R$  = low frequency resistance

$\omega / 2\pi$  = frequency

$\mu$  = magnetic permeability

$l$  = length of conductor.

the radius 0.05 cm., the permeability unity, and the specific conductivity  $2.86 \times 10^{-7}$  e.m.u. at the wave length 15 meters, we calculate a fractional increase in resistance less than 0.7%. The use of the same temperature coefficient at high frequency as at low is justified. Smith-Rose states that measurements of the conductivity of sea water between 0° C. and 40° C. indicate that the mean temperature coefficient is about 2.7% per degree centigrade. The values used in this work were about 2.4% per degree centigrade; the value varies slightly with concentration and salt.

The writer considers that the method of correcting for changes in radiation resistance is satisfactory. The reader may object, however, that  $W_0$ , the low frequency value of the carbon resistors used to determine the correction, is not the same as the true high frequency resistance  $W$  mentioned in section 2.7. If the reader be correct, the effect will be to shift the origin of coordinates on our result curves for electrolytes up or down according as  $W_0$  is less than or greater than  $W$ .

Possible errors due to non-linearity of galvanometer scale, hysteresis of galvanometer suspension, cooling of the thermocouple heater due to any cause, decrease of filament temperature of the oscillator tube, and decrease of plate potential applied to the oscillator tube are certainly negligible. The calibration of the single plate rotor of the precision condenser is believed to be correct to

0.005  $\mu\mu$ fd. This applies to the shape only of the calibration curve, its absolute position relative to the coordinate axes being without interest in this connection. The method of utilizing the entire resonance curve to determine  $\eta$  should tend to eliminate random errors in determining  $\Delta C$ , and also, the correction factor for radiation resistance eliminates entirely the units used in the calibration.

Smith-Rose found that the measured value of the conductivity of sea water at a wave length of 30 meters was essentially independent of the shape of the test cell used. However, for audio frequencies he found it necessary to correct for a polarisation film next the platinum electrodes which exhibited a capacitance of the order of a few microfarads and a resistance of the order of 100 ohms. He also noticed an effect which he attributed to the chemical action of sea water on the electrodes. No effects of this type were observed in the course of this work. We assume that the cell constants,  $k = W \sigma$ , are independent of frequency.

Chapter 5. Results

## Section 5.1 Data

The salts NaCl and MgSO<sub>4</sub> were studied at wave lengths of 45.5\*, 27.4, 16.4 and 4.04 meters. The results are shown in Figures 5.1 - 1 to 5.1 - 5. The data are all corrected to 18° C. Estimated possible errors for individual ordinates are shown by vertical lines. These errors are large enough to include (1) the error in the cell constants, (2) the error in the concentration, (3) the error in  $\Delta\eta$ , and (4) in some instances, all observations of  $\Delta\eta$ .

Curves published by Rieckhoff (who used Zahn's method) are shown (Figure 5.1 - 6) for comparison with our results. His curve for MgSO agrees well with the Debye-Falkenhagen dispersion theory.

The symbols used have the following meaning:

$\Lambda_{\omega}$  = equivalent conductivity at the frequency  $\frac{\omega}{2\pi}$ .

$\Lambda_0$  = equivalent conductivity at low frequency.

$\sigma_{\omega}$  = specific conductivity in ohm<sup>-1</sup> cm<sup>-1</sup> at the frequency  $\frac{\omega}{2\pi}$ .

$\sigma_0$  = specific conductivity in ohm<sup>-1</sup> cm<sup>-1</sup> at low frequency.

$\gamma^*$  = concentration in milligram equivalents per liter of solution.

$$\Lambda_{\omega} = \frac{10^6 \sigma_{\omega}}{\gamma^*}, \quad \Lambda_0 = \frac{10^6 \sigma_0}{\gamma^*}$$

$\lambda$  = wave length

\* At 45.5 meters wave length, circuit constants were not adjusted properly to give the same order of accuracy as at 27.4 and 16.4 meters. This was partly due to the limitation imposed by the maximum capacity of the precision condenser.

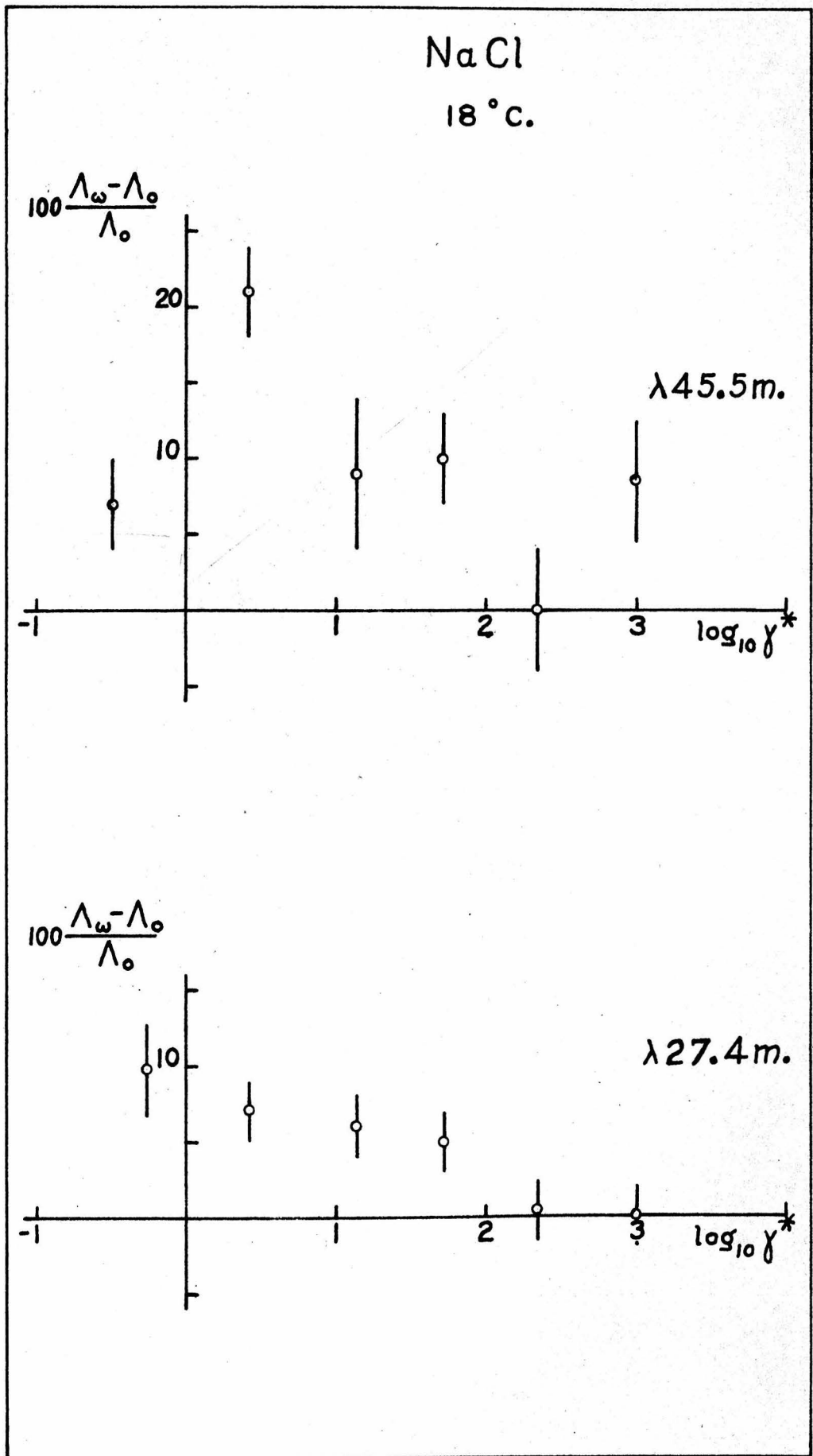


Figure 5.1-1

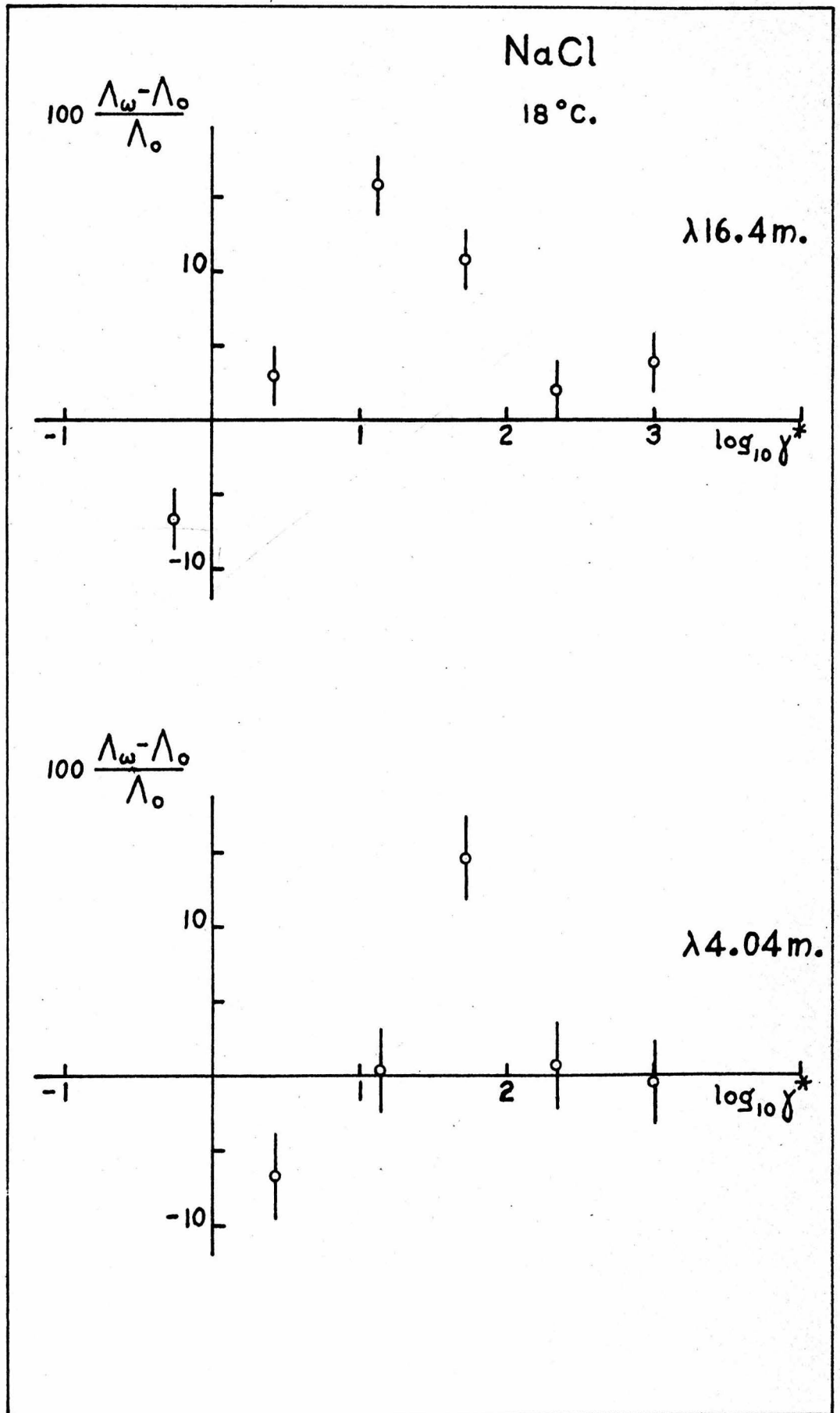


Figure 5.1-2

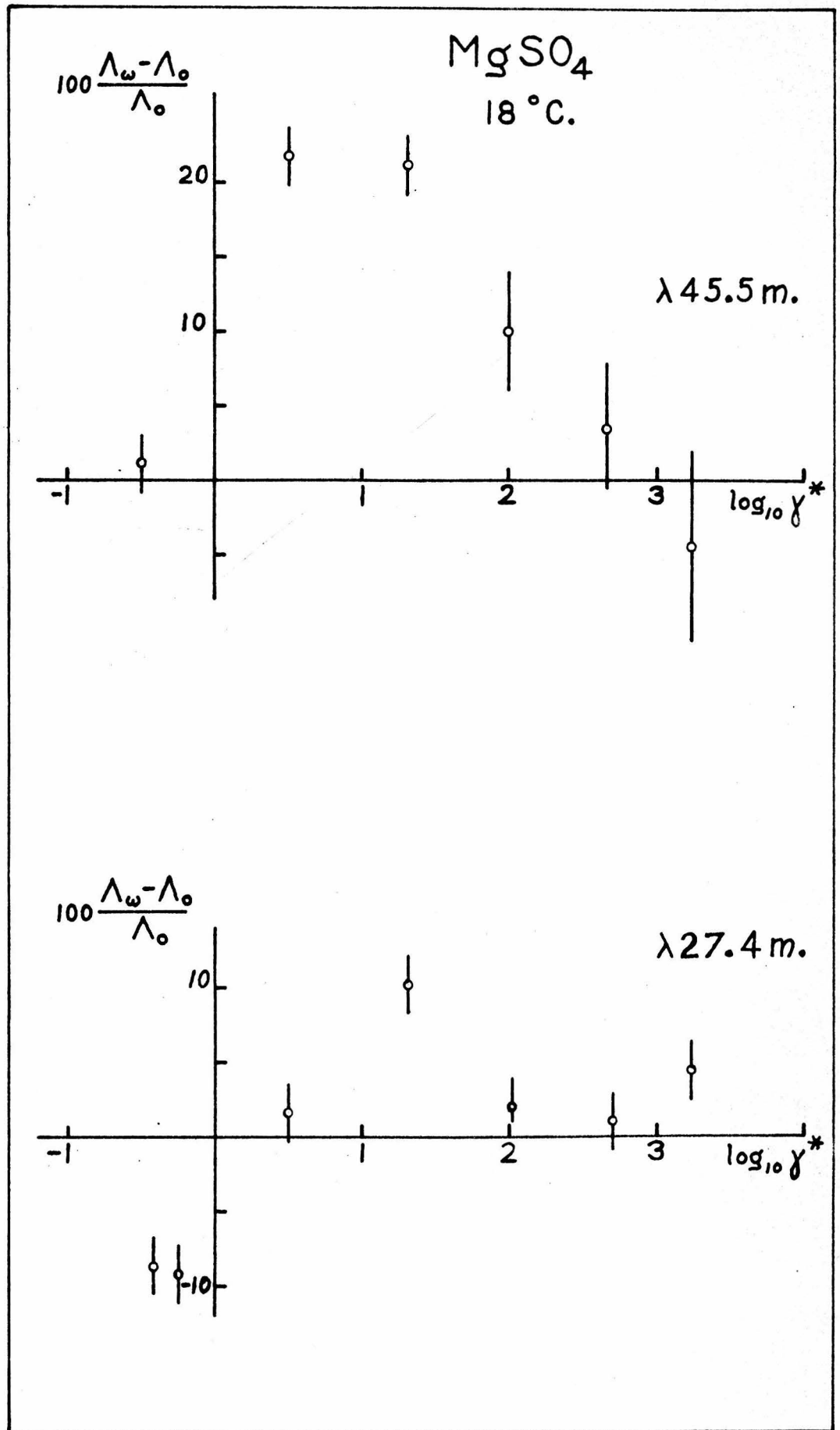


Figure 5.1-3

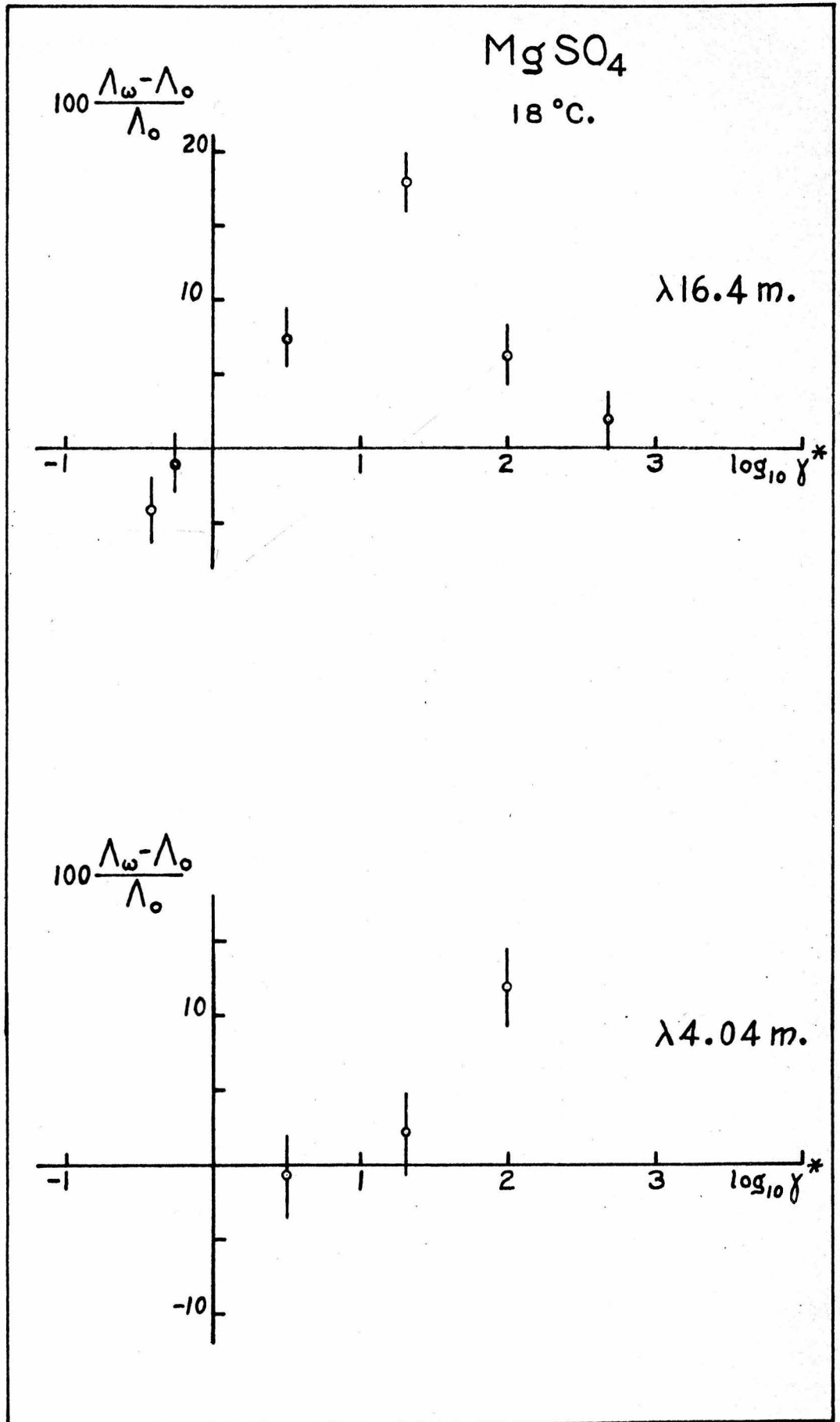


Figure 5.1-4

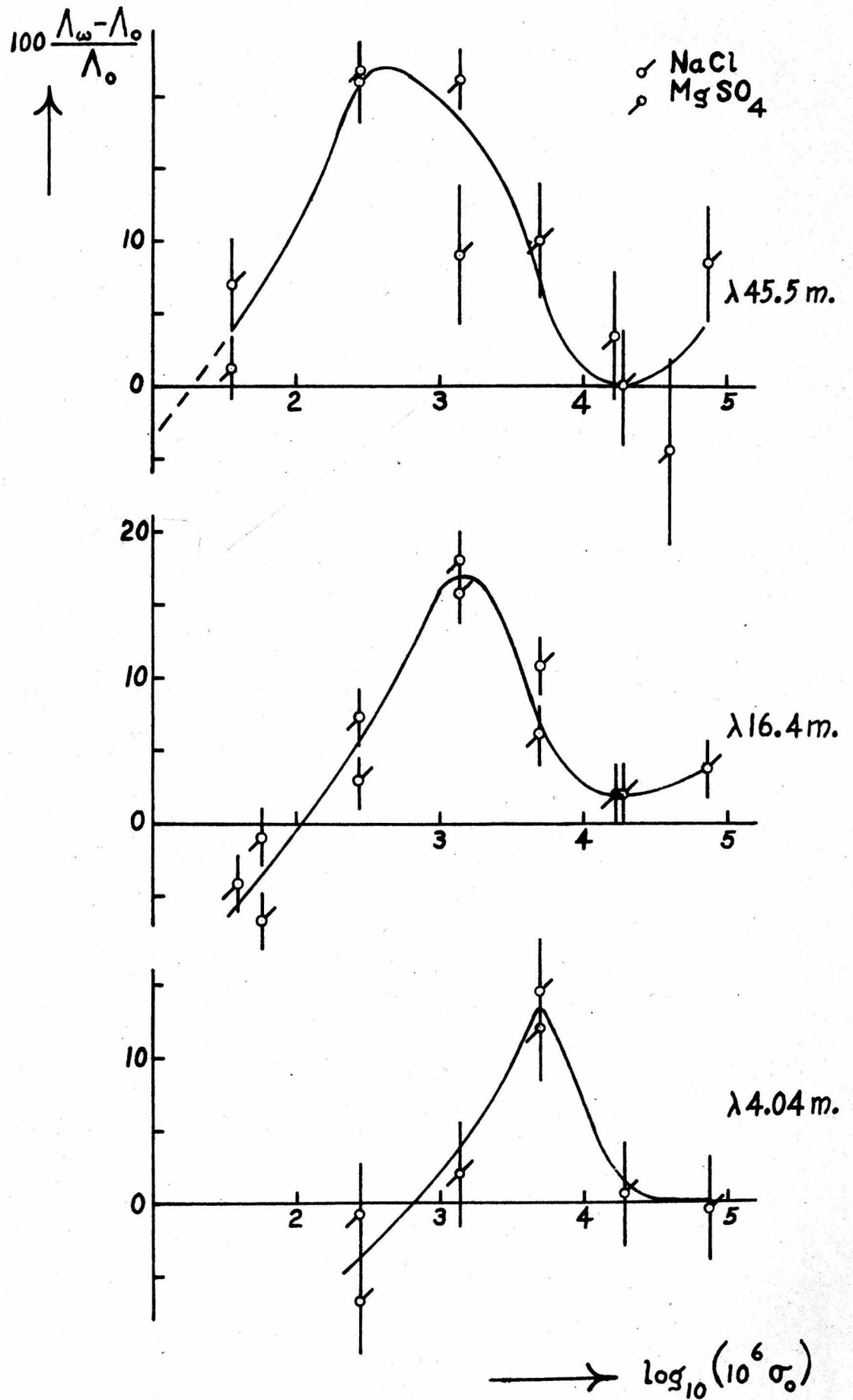


Figure 5.1 - 5

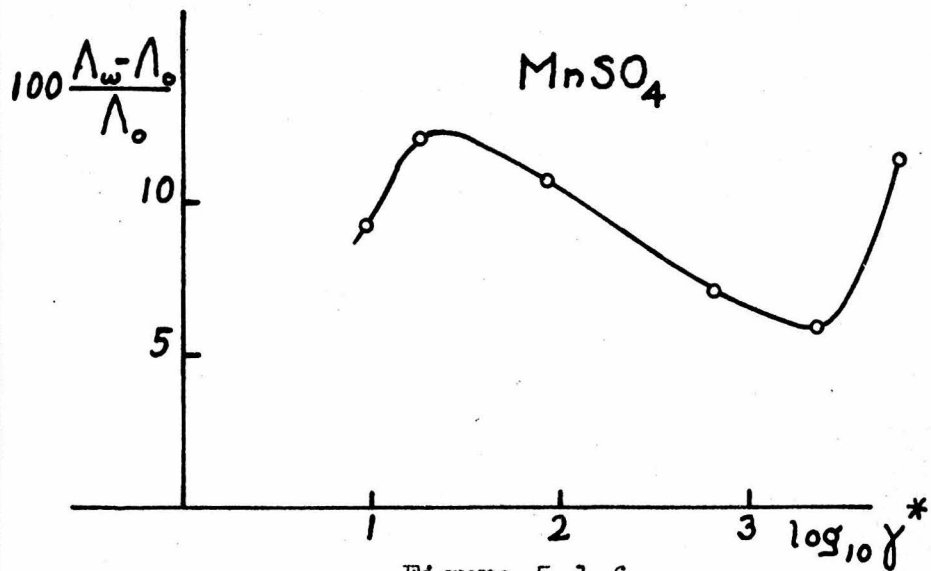
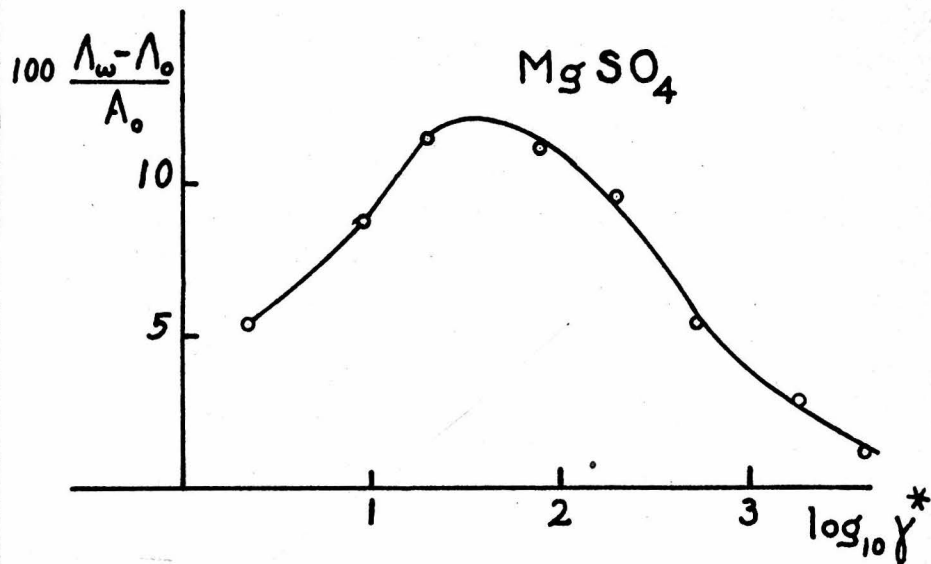


Figure 5.1-6.

These results are for a wave length of about one meter and were obtained using Zahn's method. The curves are re-plotted from a paper by Rieckhoff, Ann.d. Phys. 2 577 (1929).

## Section 5.2 Conclusions

Our conclusions are as follows:

- (1) The equivalent conductivity varies with concentration and frequency in the manner shown by the curves of section 5.1.
- (2) The results obtained disagree with the Debye-Falkenhagen theory of the dispersion of conductivity for dilute solutions of strong electrolytes; however, they do not disagree with experimental results for dilute solutions obtained by other methods.
- (3) The frequency dependence of conductivity found resembles the frequency dependence of the so-called selective heating effect. These two phenomena are, however, different in their nature. The first represents a physical property of electrolytic solutions; the second depends upon the properties of circuits used.

### Acknowledgments

To Professor G. W. Potapenko, who suggested this problem for research, my gratitude is due for his helpful criticisms and for his continued interest in the work. My thanks are due Professor W. R. Smythe, Mr. J. Pearson and Mr. B. E. Merkel for certain suggestions incorporated in the design of the precision air condensers.

## Bibliography

### I. High frequency conductivity.

1. V. Bjerknes, Ann. d. Phys. 55, 121 (1895)
2. B. Brendel, Phys. Z. 32, 327 (1931)
3. B. Brendel, O. Mittelstaedt, and H. Sack, Phys. Z. 30, 576 (1929)
4. A. Deubner, Phys. Z. 30, 946 (1929), Ann. d. Phys. 5, 305 (1930), Phys. Z. 33, 223 (1932)
5. H. Falkenhagen, Electrolytes, Clarendon Press, Oxford (1934)
6. Feldman, Proc. I. R. E. 21, 764 (1933)
7. H. Geest, Phys. Z. 34, 660 (1933)
8. W. Geyer, Ann. d. Phys. 14, 299 (1932)
9. J. Malsch, Phys. Z. 33, 19 (1932), Ann. d. Phys. 12, 865 (1932)
10. O. Neese, Ann. d. Phys. 8, 929 (1931)
11. Rayleigh, Lord, Phil. Mag. 21, 381 (1886)
12. H. Rieckhoff and Zahn, Z. Phys. 53, 619 (1929)
13. H. Rieckhoff, Ann. d. Phys. 2, 577 (1929)
14. H. Sack, Phys. Z. 29, 627 (1928)
15. H. Sack and B. Brendel, Phys. Z. 31, 345 (1930)
16. Smith-Rose, Proc. Roy. Soc. 143, 135 (1933)
17. Petrucci, N. Cimento 12, 361 (1935)
18. P. Wenk, Ann. d. Phys. 17, 679 (1933)
19. M. Wien, Ann. d. Phys. 83, 840 (1927), Phys. Z. 31, 793 (1930), Phys. Z. 32, 183 (1931), Ann. d. Phys. 11, 429 (1931)
20. H. Zahn, Z. Phys. 51, 350 (1928)

### II. Selective heating effect.

1. d'Arsonval, Comptes Rendus, Acad. Sc. 185, 324 (1927)
2. Danzer, Hochfr. 45, 85 (1935)
3. Fabry, C. R. Acad. Sc. 185, 684 (1927)
4. Hosmer, Sc. 68, 325 (1928)
5. Malov, Phys. Z. 34, 880 (1933), Hochfr. 42, 190 (1933), Z. Phys. 90, 802 (1934)
6. McLennan, Nature 126, 130 (1930)
7. McLennan and Burton, Canadian J. Res. 3, 224 (1930), 5, 550 (1931)
8. Patzold, Hochfr. 36, 85 (1930), Phys. Z. 35, 376 (1934), Strahlenther. 55, 692 (1936), Phys. Ber. 1369 (1936)